

# Numerical and Centrifuge Modelling in Soil-Structure Interaction

V.S. Chandrasekaran\*

## Introduction

In recent years numerical modelling of soil-structure interaction problems has assumed great significance not only due to the accuracy of the numerical procedures employed and easy availability of fast computers but also due to refinements achieved in characterising the strength deformation properties of the soil. Though the properties are usually evaluated under simplified experimental conditions of plane strain, axi-symmetry, simple shear or from field tests such as standard penetration test, cone penetration test or pressure meter test, they have been used extensively in solving variety of complex boundary value problems in soil-structure interaction using powerful numerical techniques. However the efficacy of the underlying methodology needs to be validated so that the procedure could be used with a greater level of confidence in practical situations.

The desirable way of achieving this would be by comparing the results of such analyses with field measurements of prototype behaviour. However opportunities for such comparisons are invariably scarce. The prediction of the performance of the structure that is to be newly built will have to be made based on a study of physical models or numerical models or both. It is in this context that studies using physical models become extremely useful. The last two decades have seen significant advances in the physical modelling of geotechnical structures using centrifuges.

---

\* Department of Civil Engineering Indian Institute of Technology Bombay, Powai, Mumbai - 400076

It should be appreciated that numerical modelling and physical modelling are complimentary technologies each contributing to the power and versatility of the other. In this paper applications of the numerical methods to problems of soil-structure interaction are first dealt with. The second part deals with the physical modelling using centrifuges. This part also includes a description of the geotechnical centrifuge facility that has been created at Indian Institute of Technology, Bombay.

## **Part I Numerical Modelling**

### **Shallow Foundations**

Three types of analytical models are commonly employed for modelling the soil behaviour.

These are :

- i) Winkler model
- ii) Elastic half-space model
- iii) Layered continuum model

#### ***Winkler model***

In this model soil mass is replaced by a bed of infinitesimally close independent springs. The shear resistance in the soil is neglected thus ignoring the continuity present in the soil mass. The soil outside the loaded area does not undergo any deformation. The soil stiffness is characterised by the modulus of subgrade reaction  $k_s$  defined by the equation

$$\frac{p}{v} = k_s \quad (1)$$

Where  $p$  is the intensity of load transmitted to the soil and  $v$  is the consequent deflection. The flexure of a beam resting on such a medium is governed by the differential equation

$$EI \frac{d^4 v}{dx^4} = -kv + q \quad (2)$$

where  $k_s$  is the modulus of subgrade reaction,  $k$  is equal to  $k_s B$  where  $B$  is the width of the foundation,  $v$  is the vertical deflection at

any point  $x$ ,  $q$  is the applied loading per unit length at  $x$  and  $EI$  is the flexural rigidity of the beam. A large number of papers are available in the literature for the solution of Eq.2 (Eg. Hetenyi 1946, Bowles 1988 )

While Winkler beam analysis has now become straightforward the choice of appropriate value of modulus of subgrade reaction still remains a puzzle with engineers. Terzaghi (1955) proposed simple formulae for obtaining the subgrade modulus for rectangular foundations of different sizes based on plate load test data for different soil types. His recommendations have been widely quoted in the literature and used in practice. These proposals take into account effect of the size of foundation in the settlement, based on stress distribution and pressure bulbs obtained in elastic half-space models.

Vesic (1969) proposed the following relationship for computing the value of modulus of subgrade reaction in the analysis of relatively flexible beams :

$$k = k_s B = 0.65 \sqrt[12]{\frac{E_s B^4}{E_b I} \frac{E_s}{1 - \nu_s^2}} \quad (3)$$

where

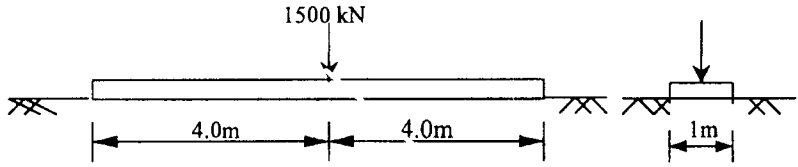
$E_s$  = Modulus of elasticity of soil

$\nu_s$  = Poisson's ratio of soil

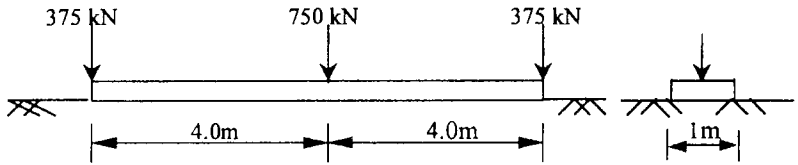
$E_b I$  = Flexural rigidity of the beam

He recommended that if a value of modulus of subgrade reaction based on Eq.3 is used then the results of analyses of Winkler beam and elastic half-space beam would be practically the same. On the face of it, the proposal looks attractive as the complex analysis of the beam resting on an elastic half-space could be replaced by a simpler Winkler beam analysis. The drawbacks of Vesic's recommendation are illustrated below:

Two problems have been considered; one, a beam subjected to central loading and another, the same beam subjected to three-point loading. The properties of the beam and the soil are given in Fig.1. The total load is the same in both cases equal to 1500kN. For the Winkler analysis the value of  $k$  was calculated using Eq.3. The characteristic length  $\lambda L$  for the beam is calculated as 2.75m which is greater than 2.5 satisfying the criterion set by Vesic. The summary of the results are



(a) Single Point Loading



(b) Three Point Loading

$$E_s = 15264.0 \text{ kN/m}^2, \nu_s = 0.2,$$

$$E_b I = 152000 \text{ kN.m}^2$$

$$k_{(\text{vesic})} = 8533.54 \text{ kN/m}^3$$

FIGURE 1 : Loading Diagram of Beam

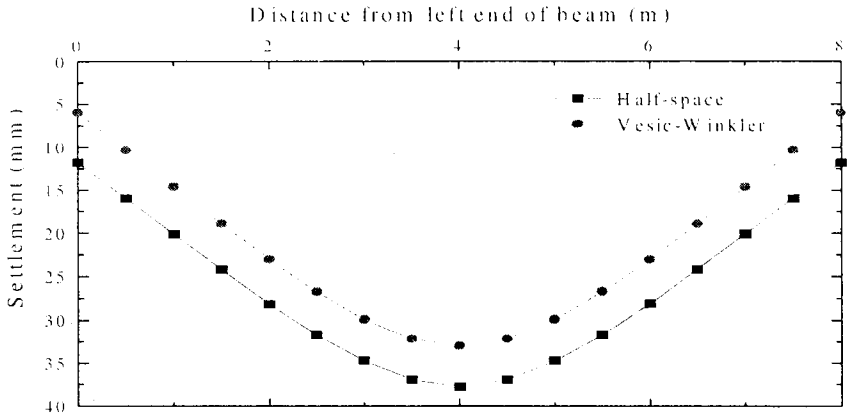


FIGURE 2 : Comparison of Settlement Diagrams for Single Point Loading

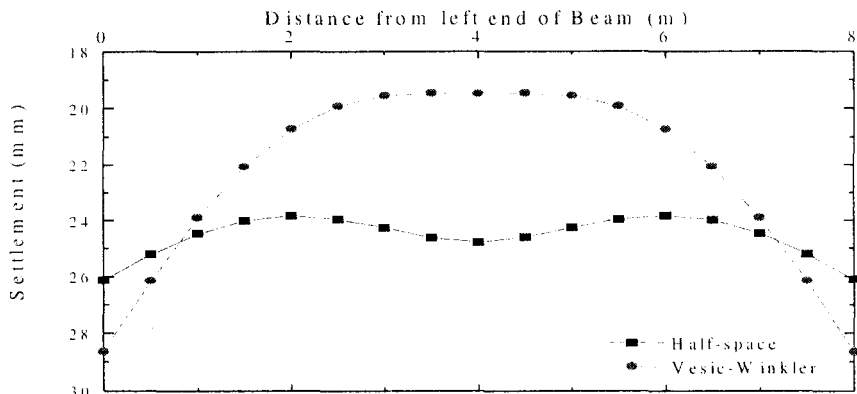
given in Table 1. For the single point loading the bending moment and the differential settlement between centre and edge match well between half-space and Vesic-Winkler beam even though the settlement of Vesic-Winkler beam is less than that of half-space beam. This is illustrated in Fig.2. For the three point loading, the comparison of elastic half-space and Vesic-Winkler beam solutions are shown in Fig.3. In problems of soil-structure interaction the damage criterion is based on the angular distortion defined by the ratio of differential settlement to the spacing between the columns. Table 1 clearly illustrates the inadequacy of the Vesic's formula in this respect. The values of bending moments also do not match. Vesic's formula was derived for single central loading on a beam and can not model the behaviour, when multiple loads are present. It may be concluded that there is no merit in trying to idealise a half-space beam analysis by a Winkler beam analysis based on Vesic's recommendation. Such an analysis will not capture the angular distortion which is the principal factor of damage criteria of buildings. With proven numerical methods of analysis for half space problems now becoming available, there is no benefit to be derived by following Vesic's approach.

Winkler model for soil is proven only in the case of Gibson soil medium where the elastic modulus is proportional to depth and the Poisson ratio is equal to 0.5. There will be only limited application of this in practice.

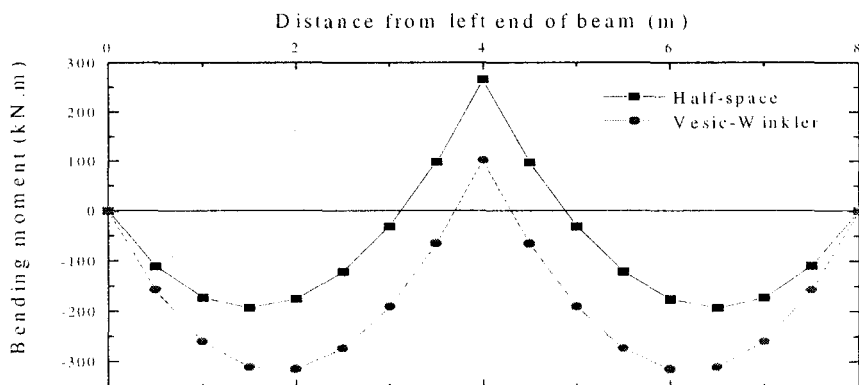
**Table 1 : Comparison of Vesic-Winkler and Half-space Beam Analyses**

Loading	Beam Thickness (mm)	$w_c$ (mm)	$w_e$ (mm)	$\delta = (w_c - w_e)/L$	Max. Positive Bending Moment (kN.m)	Max. Negative Bending Moment (kN.m)
Single point	400	5.99	33.05	1 / 148)	1171.0	-
		(11.80)	(37.76)	(1 / 154)	(1132.0)	-
	500	13.41	30.00	1 / 242	1310.0	-
		(15.97)	(33.28)	(1 / 231)	(1333.0)	-
Three point	400	28.66	19.52	- 1 / 438	101.5	314.0
		(26.11)	(24.78)	(- 1 / 3008)	(266.0)	(192.7)
	500	27.23	21.68	- 1 / 720	58.9	340.2
		(25.57)	(24.61)	(- 1 / 4167)	(257.2)	(202.3)

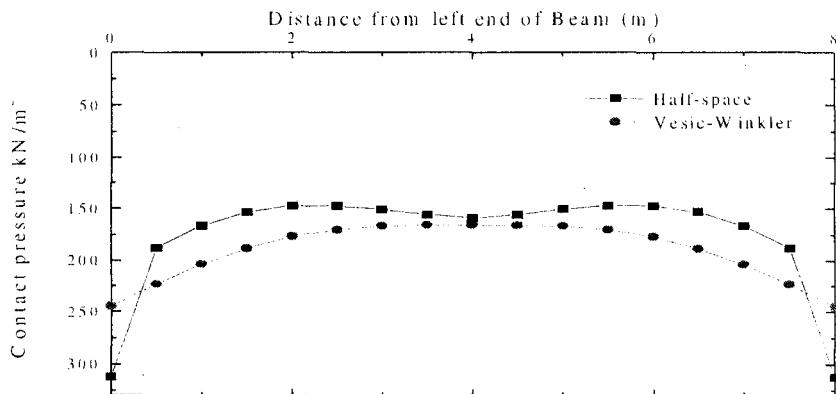
Figures in brackets pertain to half-space model.



(a) Settlement diagram



(b) Bending moment diagram



(c) Variation of contact pressure

**FIGURE 3 : Comparison of Half-space and Vesic-Winkler Beam Analyses for Three Point Loading**

### *Elastic half-space model for soil*

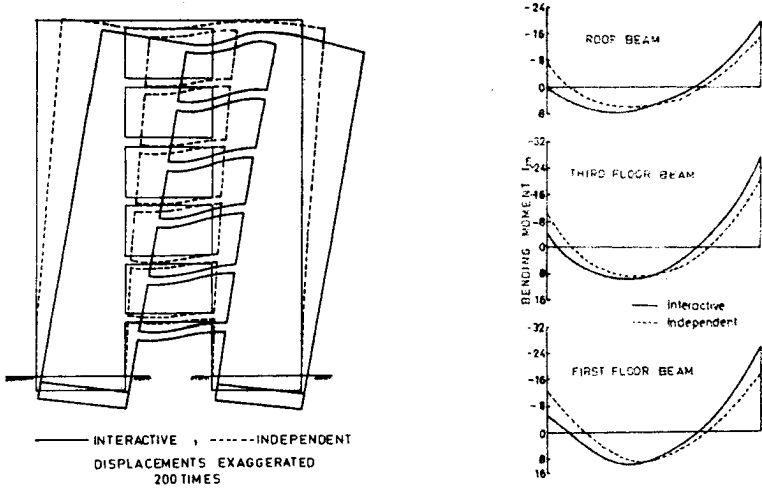
The elastic half-space model for soil is superior to the Winkler medium inasmuch as the continuity present in the soil medium is accounted for in the model. Another advantage of the model is its versatility in transferring horizontal shear stresses beneath the foundation. Presently the methods of analysis based on obtaining the support stiffness of elastic half-space have been dealt with by Cheung and Nag (1968) for beams and Cheung and Zienkiewicz (1965), Svec and McNiece (1972) and Buragoin and Shah (1981) for rafts. If the soil behaves elastically then undrained modulus  $E_u$  and Poisson's ratio equal to 0.5 will model the immediate behaviour. On the other hand the drained elastic parameters  $E'$  and  $\nu'$  could be used for modelling the long-term behaviour.

Application of the half-space model in analysing the interaction of the shear wall with openings with the footing foundations having adhesive contact resting on an elastic half-space is illustrated in Fig.4. (Chandrasekaran and Khedkar,1977). Plane stress finite element elastic model was used for the shear wall and the half-space stiffness was obtained using Cheung and Nag (1968) approach. It may be seen that in this case, consideration of structure foundation interaction gives rise to a larger horizontal displacements and changes in the stress resultants of the super-structure lintel beams. Concentration of horizontal shear stress in the footing edges indicates the right place to provide shear keys if they are envisaged.

## **Layered or Inhomogeneous Soil Medium**

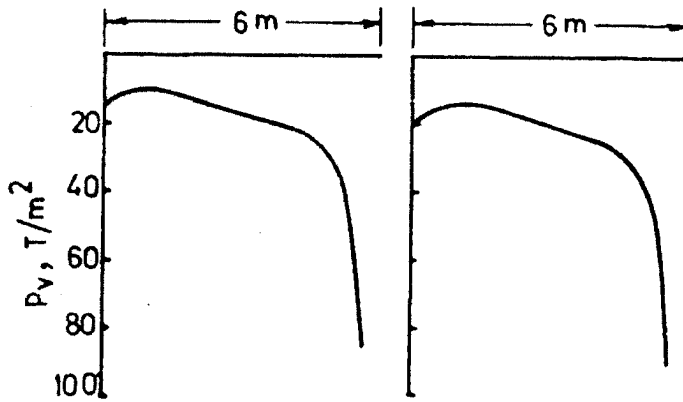
### *Finite element model*

In practical situations the soil medium is rarely homogeneous and the stress distribution may not be akin to that obtained using homogenous elastic half-space model. In recent years the finite element method has been developed to a high degree of refinement to model the soil behaviour. An illustrative example is presented here (King and Chandrasekaran, 1974, 1977) involving finite element modelling of soil raft and space frame. The building elevations and the plan of the raft are shown in Fig.5. Here the undrained parameter  $E_u$  and  $\nu_u$  and drained parameters  $E'$  and  $\nu'$  were used for simulating the immediate and long term behaviour respectively. The variation of  $E_u$  and  $E'$  with depth is shown in Fig.6 the finite element idealisation of the raft and soil the medium is shown in Fig.7. The results are discussed along with those of the simplified soil model.

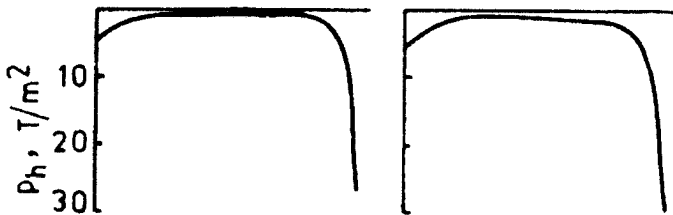


a. Displacement profiles for interactive and independent analysis

b. Bending moment diagrams for lintel beams

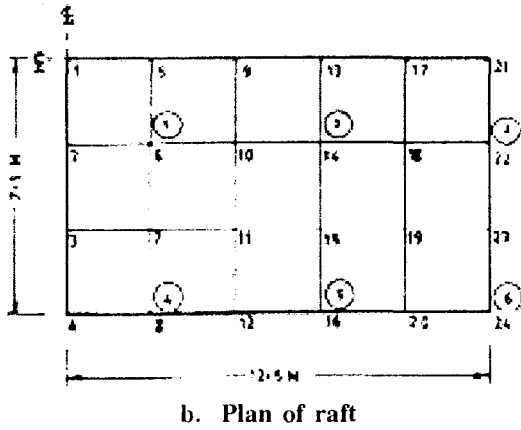
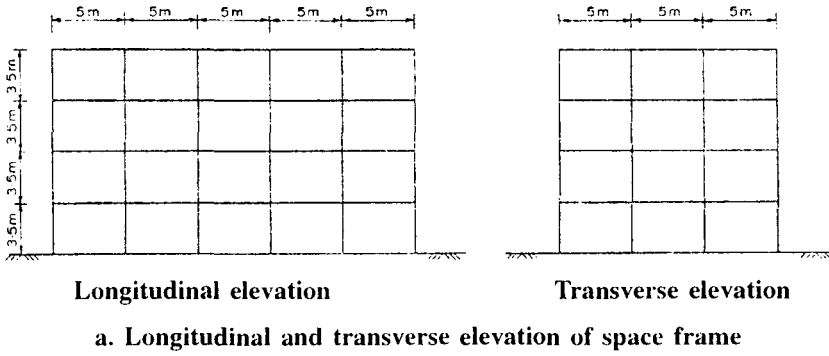


c. Vertical contact pressure distribution

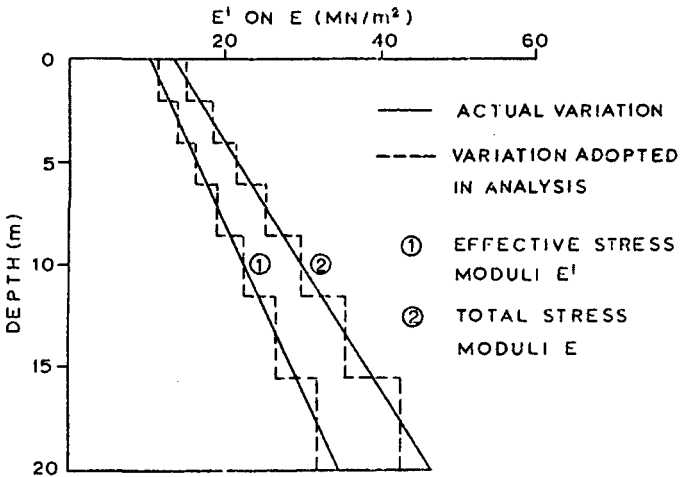


d. Horizontal contact pressure distribution

FIGURE 4 : Shear Wall Foundation Interaction



**FIGURE 5 : Space Frame and Raft**



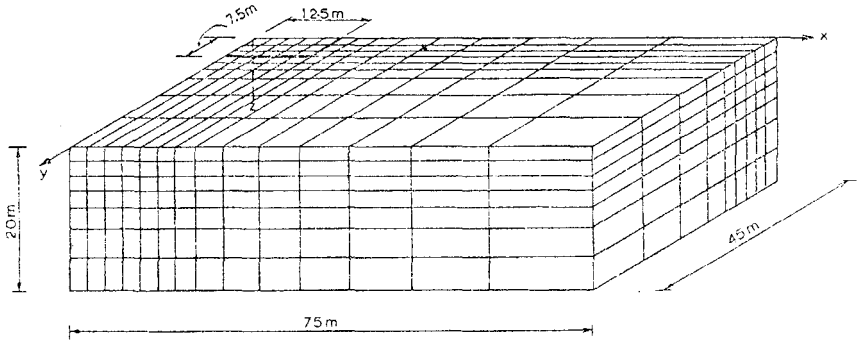


FIGURE 7 : Finite Element Idealization of Raft and Soil Medium

### *Simplified soil model*

One simplification which is often resorted to is to assume Boussinesq's stress distribution in the medium and compute the vertical strains based on variable elastic modulus. If one follows (Skempton's and Bjeurrum, 1957) approach the immediate and consolidation settlements may be computed as

$$s_{imm} = \sum_{r=1}^n \frac{1}{E_{ur}} [\sigma_{zi} - 0.5(\sigma_{xi} + \sigma_{yi})] \quad (4)$$

$$s_{cons} = \sum_{r=1}^n u_{ir} m_{vr} \cdot H_r \quad (5)$$

$$s_{final} = s_{imm} + s_{cons} \quad (6)$$

$\sigma_{xi}$ ,  $\sigma_{yi}$  and  $\sigma_{zi}$  are the immediate normal stresses in the coordinate directions,  $u_i$  is the immediate pore pressure,  $E_{ur}$  is the undrained elastic modulus of the  $r^{th}$  layer,  $m_{vr}$  is the coefficient of volume compressibility of the  $r^{th}$  layer and  $H_r$  is the thickness of the  $r^{th}$  layer.

Where  $u_i$  is the immediate pore pressure which, in the case of isotropic elastic medium may be obtained from the relationship.

$$u_i = \frac{\sigma_{xi} + \sigma_{yi} + \sigma_{zi}}{3} \quad (7)$$

If the soil shows high compressibility as will be the case for lightly over consolidated and normally consolidated soils then the pore pressure

may be computed from Skempton's pore pressure equation ignoring the effect of the rotation of principal stress. Method of obtaining the raft support stiffness based on the above has been described by King and Chandrasekaran (1977).

The same problem illustrated in Fig. 5 was analysed using this procedure. The variation of  $m_v$  with depth is shown in Fig. 8. Table 2 give the results of settlements of column bases and differential settlement between columns obtained from interactive analysis by considering the

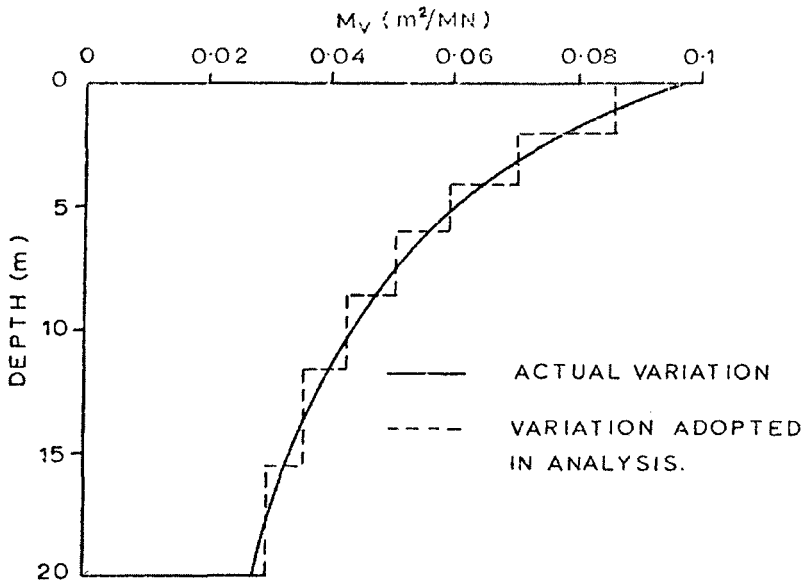


FIGURE 8 : Variation of  $m_v$  with Depth

mutual interaction of soil, foundation and superstructure. Table 3 gives the loads transferred by the columns to the raft. The results cover finite element model for the soil medium and the simplified soil model. Both short term and long term settlements are considered. For this case the results based on the simplified soil model are acceptable. The simplified soil model has the merit of using simple soil properties such as  $E_u$  and  $m_v$ . However, an understanding of the stress flow (distribution) through the soil medium will enable engineers to assess the efficacy of using simple soil model. Total and differential settlements can be estimated realistically only by proper modelling the soil support for immediate and long term behaviour.

**Table 2. Comparison of Settlements and Differential Settlements**

Settlement	Isotropic			
	Immediate		Long Term	
$s_1$	19.8	(25.2)	46.5	(49.7)
$s_2$	17.8	(22.5)	41.7	(44.6)
$s_3$	12.4	(15.7)	31.5	(34.3)
$s_4$	14.0	(18.2)	36.5	(39.9)
$s_5$	12.6	(16.3)	32.7	(35.8)
$s_6$	8.6	(11.3)	24.7	(27.9)
$\delta_{1,2}$	2.0	(2.7)	4.8	(5.1)
$\delta_{2,3}$	5.4	(6.8)	10.2	(10.3)
$\delta_{4,5}$	1.4	(1.9)	8.0	(4.1)
$\delta_{5,6}$	4.0	(5.0)	8.0	(7.9)
$\delta_{1,4}$	5.8	(7.0)	10.0	(9.8)
$\delta_{2,5}$	5.2	(6.2)	9.0	(8.8)
$\delta_{3,6}$	3.8	(4.4)	6.8	(6.4)

All settlement values are in mm

Values in brackets pertain to finite element idealisation of soil

$s_i$  : Settlement of column  $i$

$\delta_{ij}$  : Differential settlement between columns  $i$  and  $j$

**Table 3. Comparison of Column Forces Transferred to Raft**

Forces or Moments	Independent Analysis	Interactive Analysis			
		Immediate		Long Term	
$P_1$	1257.5	1177.8	(1156.4)	1099.1	(1096.7)
$P_2$	1265.7	1151.1	(1130.2)	1077.1	(1085.6)
$P_3$	610.6	626.3	(634.1)	643.2	(646.0)
$P_4$	607.1	672.3	(682.8)	706.1	(699.7)
$P_5$	608.1	633.1	(641.3)	660.8	(665.1)
$P_6$	301.0	389.4	(405.1)	463.7	(457.0)

All values are in kN

Values in brackets pertain to finite element idealisation of soil

## Caissons

In order to analyse structures founded on a deep foundations it is necessary to assess their response to different types of loading such as vertical and lateral. These responses are governed not only by the stiffness and strength of the soil support but also by the stiffness of the foundation element. Foundation such as caisson or large diameter pier acts like a rigid element embedded in the soil medium whereas long piles act as relatively flexible members embedded in the soil medium. We shall confine our discussion to response under static loading only. Response of caissons are considered first and then piles are discussed. For the sake of simplicity it is assumed that they have circular cross section.

Though the soil support on the sides and the base is frequently modelled by means of springs using subgrade reaction theory such an approach for caissons is riddled with inaccuracies. For rigid and large objects such as caissons, there will be considerable interaction between the side resistance and base resistance and discrete springs on the sides and on the base can not account for this interaction satisfactorily. A better approach will be to model the soil medium as a continuum and we shall consider that to be elastic.

The general loading may be resolved into four components consisting of an axial force, a resultant lateral force, a resultant lateral moment and torsion about the axis of geometric symmetry. Only axial and lateral loadings are considered. When the soil property remains constant in the circumferential direction the axial component of the load will produce stresses and displacements which are axi-symmetric. On the other hand, lateral force and lateral moment will produce stresses and displacements which are three-dimensional in nature.

Three approaches are available for analysing a Caissons embedded in an elastic continuum : (i) procedures based on Mindlin's equation for homogenous elastic half-space (ii) boundary element method and (iii) finite element method. The first approach which is based on integration of Mindlin's solution suffers from a drawback, that the presence of the foundation element in the soil medium is ignored in the analysis. The second approach presents considerable difficulties when inhomogeneities are present or when interface friction needs to be modelled. The author considers that analyses based on finite element method have a number of advantages in respect of consideration of inhomogeneous soil and modelling of interface behaviour and non-linearity.

### *Finite element formulation for caisson and soil*

If the soil properties do not vary in the circumferential direction, axial loading can be studied using axi-symmetric finite element formulation which reduces to a two dimensional analyses. On the other hand lateral loading gives rise to three dimensional deformation in the soil medium requiring three dimensional finite element analysis. However three dimensional analysis could be reduced to a number two dimensional analysis by using a formulation known as semi-analytical finite element formulation (Wilson 1965). For the case of lateral loading the displacements are represented by

$$\left. \begin{aligned} u &= \sum_{n=1}^N \bar{u}_n \cos n\theta \\ v &= \sum_{n=1}^N \bar{v}_n \cos n\theta \\ w &= \sum_{n=1}^N \bar{w}_n \sin n\theta \end{aligned} \right\} \quad (8)$$

Where  $u$ ,  $v$ ,  $w$  are displacements in radial, vertical and circumferential directions and  $\bar{u}$ ,  $\bar{v}$  and  $\bar{w}$  are the amplitudes of displacement in the corresponding directions.  $N$  represents number of harmonics considered in the analysis. A special element for modelling the interface on the sides and base based on semi-analytical formulation is presented by Desai( 1982 ).

### *Influence coefficients*

The finite element discretization shown in Fig. 9 illustrates a caisson foundation embedded in a soil medium. Axisymmetric finite element formulation was used in the case of axial loading and semi-analytical finite element formulation was used in the case of lateral loading. Consider the caisson foundation shown in Fig. 10. Influence coefficients were obtained for vertical, horizontal and rotational displacements at the top of the caisson for the cases where the medium has a constant elastic modulus equal to  $E_s$  or where the elastic modulus varies with depth according to the equation  $E_s = mz$ . The results are presented in the

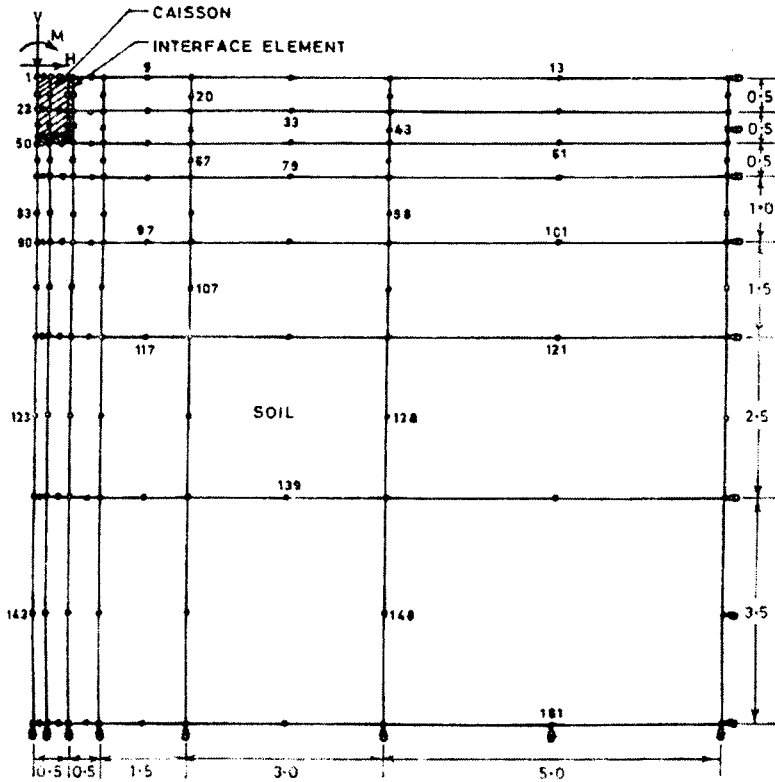


FIGURE 9 : Finite Element Discretization for Caisson

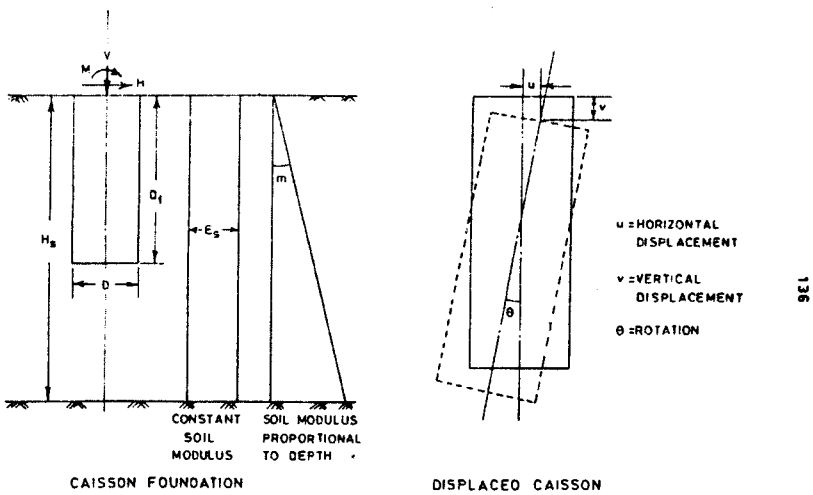


FIGURE : 10 Caisson Foundation and its Displaced Configuration

form of influence coefficients which are defined in Table 4. The influence coefficients are presented for various values of  $D_f/D$  and  $H_s/D_f$  in Figs. 11 to 15. These figures pertain to a Poisson's ratio value of 0.47. The problem of no contact tension and non-linear behaviour of soil are dealt with by Desai and Chandrasekaran (1985, 1993).

## Axially Loaded Piles

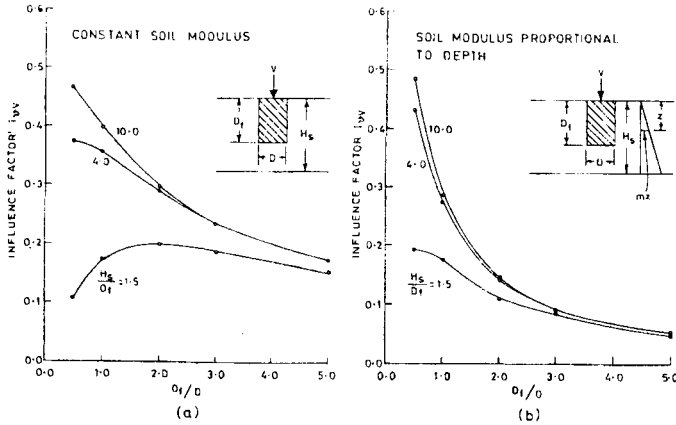
Pile head displacement under axial load may be obtained directly from a pile load test which will give the displacement for the duration of the test. Analytically the pile head displacement may be estimated by the following approaches; (i) by treating the soil medium as a homogeneous elastic half space (Eg. Poulos and Davis, 1968) (ii) from a finite element analysis using non-linear stress-strain relationship for the soil and the interface (Eg. Chandrasekaran and Ambadekar 1983) and (iii) from  $\tau$ -w analysis in which the shaft support and base support are modelled using non-linear springs. The second and third methods have the attributes that they can account for variable properties of soil deposits. The finite element formulation of the third method as proposed by Chandrasekaran et al. (1987) is briefly described here. Based on the

**Table 4. Definition of Non-Dimensional Influence Coefficients**

Loading	Disp.	$E_s = \text{Const.}$	$E_s = mz$
Vertical	Vertical	$u_v = \frac{I_{vv} V}{E_s D}$	$u_v = \frac{I_{vv} V}{m D^2}$
Horizontal	Horizontal	$u_h = \frac{I_{hh} H}{E_s D}$	$u_h = \frac{I_{hh} H}{E_s D^2}$
Horizontal	Rotational	$\theta_{hh} = \frac{I_{hh} H}{E_s D^2}$	$\theta_{hh} = \frac{I_{hh} H}{m D^3}$
Moment	Horizontal	$u_M = \frac{I_{uM} M}{E_s D^2}$	$u_M = \frac{I_{uM} M}{E_s D^3}$
Moment	Rotational	$\theta_M = \frac{I_{\theta M} M}{E_s D^3}$	$\theta_M = \frac{I_{\theta M} M}{m D^4}$

v = vertical displacement  
u = lateral displacement  
 $\theta$  = rotational displacement in radian  
V = vertical load  
H = horizontal load

$M$  = moment  
D = diameter of caisson  
 $E_s$  = elastic modulus of soil  
m = rate of variation of  $E_s$  with depth



871

FIGURE 11 : Influence Coefficients for Vertical Loading

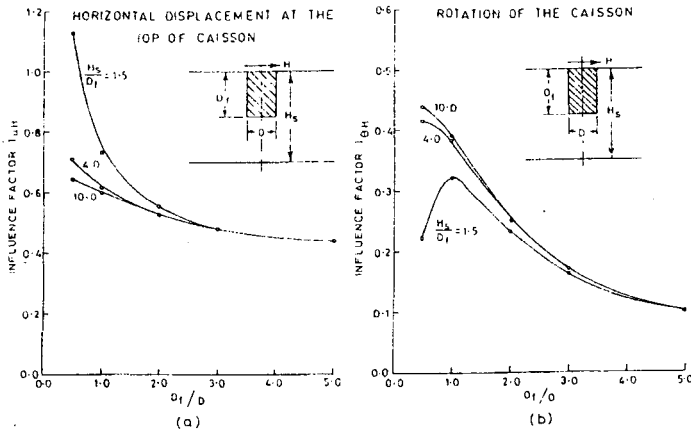


FIGURE 12 : Influence Coefficients for Horizontal Loading ( $E_s$  constant)

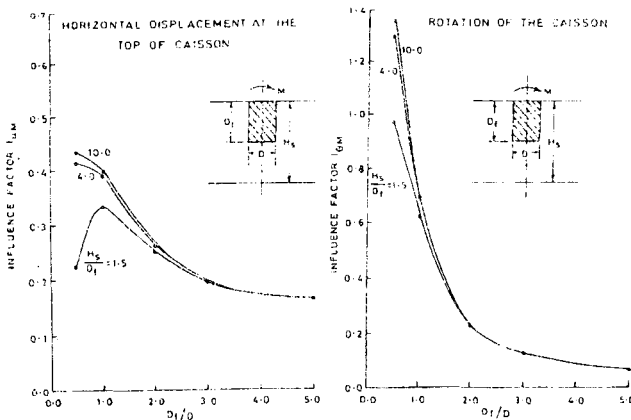


FIGURE 13 : Influence Coefficients for Moment Loading ( $E_s$  constant)

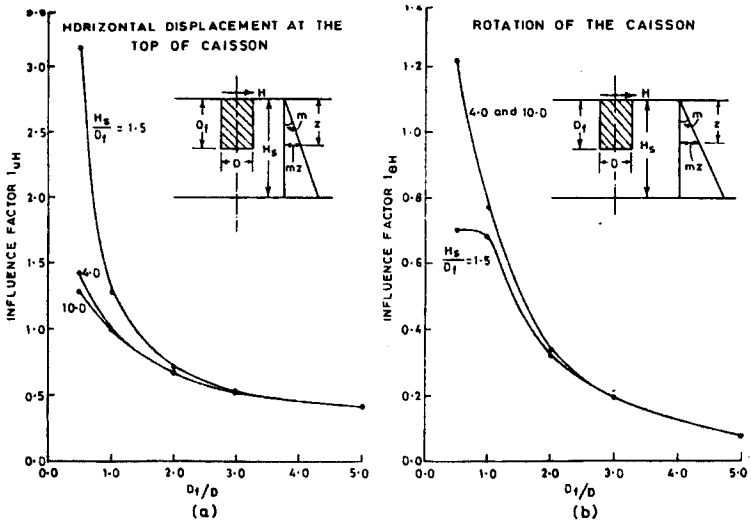


FIGURE 14 : Influence Coefficients for Horizontal Loading ( $E_s = mz$ )

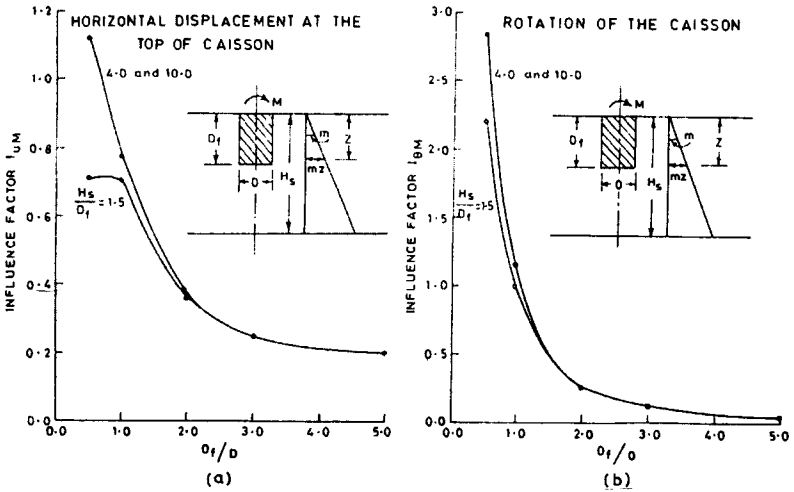


FIGURE 15 : Influence Coefficients for Moment Loading ( $E_s = mz$ )

assumption of radial transfer of shear stress and following the approach proposed by Randolph and Wroth (1978) (see Fig.16) the stiffness of the springs providing the shaft resistance is given by

$$k = \frac{2\pi r_0 \tau_s}{w_s} = \frac{2\pi G}{\zeta} \tag{9}$$

where  $k$  = stiffness of soil spring,  $r_0$  = radius of pile.

$\tau_s$  = skin friction,  $G$  = shear modulus of soil along the side of pile and  $\zeta = \ln \frac{r_m}{r}$  where  $r_m$  is the radius at which the vertical soils displacement along  $r$  radius becomes negligible. An average value of  $\zeta$  equal to 4 is frequently recommended. Other proposals have given by Randolph and Wroth (1978). If the ultimate skin friction is known, then a non-linear  $\tau_s$ - $w_s$  relationship could be arrived at. Two such proposals are given in Fig. 17. Stiffness of base spring may be assumed according to rigid punch solution on the surface of homogenous elastic half-space given by

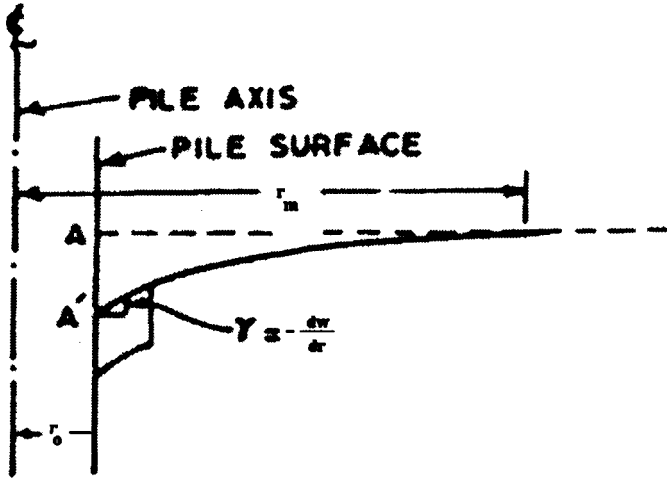


FIGURE 16 : Shear Transfer Near Pile Shaft

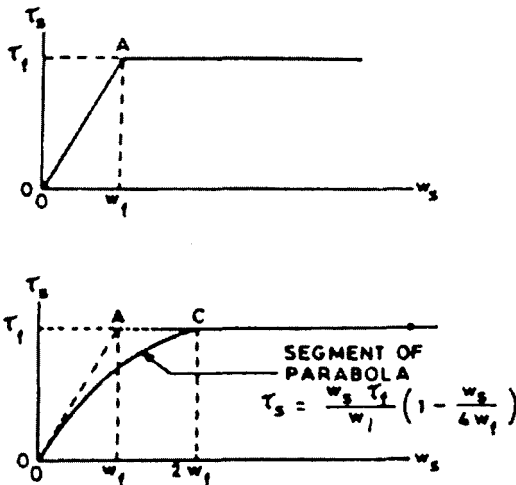


FIGURE 17 : Bilinear and Parabolic Models for Skin Friction

$$\frac{q_b}{w_b} = \frac{2r_b E_b}{(1 - \nu_b^2)} \quad (10)$$

where  $q_b$  = load transmitted at the base,  $w_b$  = pile base displacement  
 $r_b$  = radius of the base,  $E_b$  = elastic modulus of the soil at the base and  
 $\nu_b$  = Poisson's ratio of soil at the base. If the ultimate base resistance  
 can be estimated, a suitable non-linear base spring stiffness could be  
 estimated. The finite element formulation for the pile analysis is given  
 below.

### *Finite element formulation*

The pile is discretized into a number of elements as shown in Fig.18.  
 A linear variation of axial displacement between the nodes is assumed  
 in the formulation. The axial deformation of the element is resisted by  
 skin friction which is modelled by springs with stiffness varying linearly  
 over the depth from  $k_{si}$  to  $k_{sj}$ . The force-displacement relationship of  
 such an element may be obtained by following the principle of virtual  
 work in the form :

$$\begin{Bmatrix} F_i \\ F_j \end{Bmatrix} = [K]_k \begin{Bmatrix} u_i \\ u_j \end{Bmatrix} \quad (11)$$

$$[K]_k = \frac{AE}{L} \begin{bmatrix} 1 & -1 \\ -1 & 1 \end{bmatrix} + cLK_{si} \begin{bmatrix} \frac{1}{4} & \frac{1}{12} \\ \frac{1}{12} & \frac{1}{12} \end{bmatrix} + cLK_{sj} \begin{bmatrix} \frac{1}{12} & \frac{1}{12} \\ \frac{1}{12} & \frac{1}{4} \end{bmatrix} \quad (12)$$

in which A is the area of cross section, c and L are the perimeter and  
 element length and E is the elastic modulus of the material of the pile.  
 The stiffness matrices of all the shaft elements are assembled and the  
 base stiffness of soil added on to the bottom node. The resulting set of  
 linear simultaneous equations may then be solved to obtain the axial  
 displacements of the nodes under the externally applied loads at pile  
 head. Since, the  $\tau_s - w_s$  and  $q_b - w_b$  relationships are non-linear, an  
 interactive procedure would be needed for the solution of the equations.  
 The secant modulus approach was adopted in the present analysis and a  
 special computer program was developed to facilitate interpretation and  
 back analysis of test data.

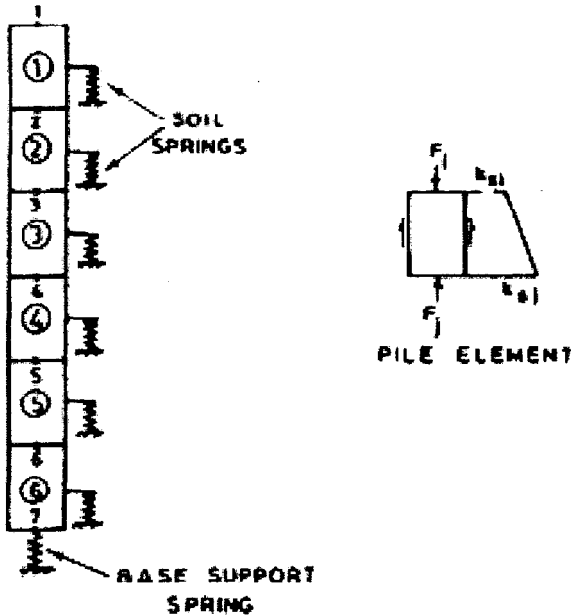


FIGURE 18 : Finite Element Discretization of Pile and Modelling of Soil Support

*Back analysis of pile load tests*

Results of pile load tests carried out at Manali near Chennai in Tamil Nadu and at Haldia in West Bengal were considered for back analysis. The soil profile at the Manali site along with the SPT data is shown in Fig.19. The test piles at Manali site, designated as MTP1 and MTP3, were 40.64 cm and 33.02 cm in diameter respectively and had been driven to a depth of 14.0 m below the ground level. The soil profile at the Haldia site is shown in Fig.20. The test piles at this site, designated as HTP1 and HTP3 were both 56 cm in diameter and of bored, cast-in-situ type. Bentonite slurry was used during drilling. The tip of the pile HTP1 was located in the dense sand layer at a depth of 39.6 m and an SPT test conducted at the bottom of the borehole prior to concreting indicated  $N_{60}$  to be of the order of 74. The test pile HTP3 was terminated at a depth of 53.6m, the  $N$ -value at the tip level being more than 50. The  $t_s / w_s$  and  $t_b / w_b$  relationships used in the analyses are given by Chandrasekaran et al. A comparison of the results of the four pile load tests and those computed on the basis of bilinear and parabolic models for soil support is shown in Figs. 21 to 24. It may be noted that there is reasonable agreement between the observed and computed results.

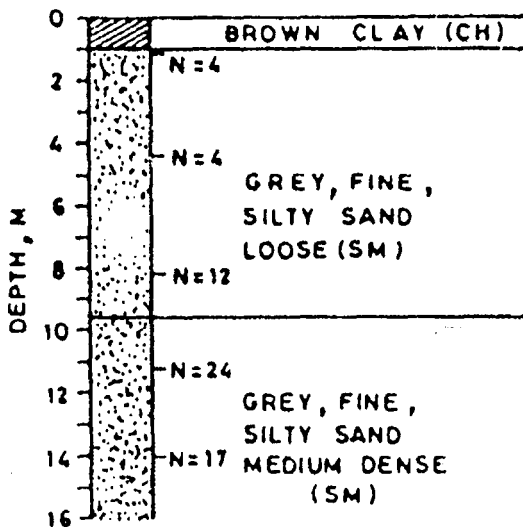


FIGURE 19 : Soil Profile at Manali Site

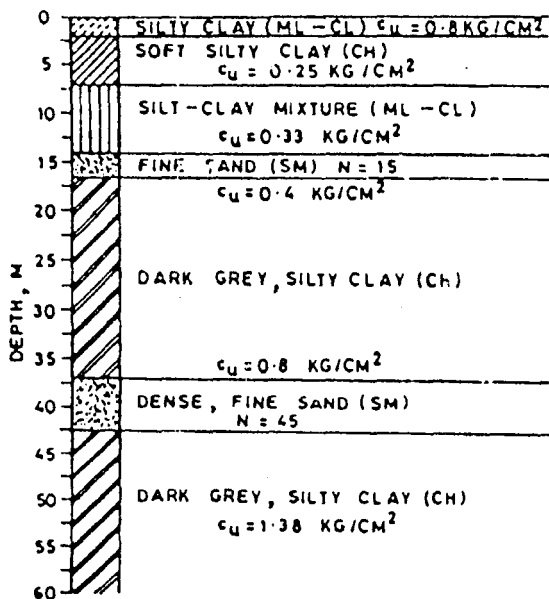


FIGURE 20 : Soil Profile at Haldia Site

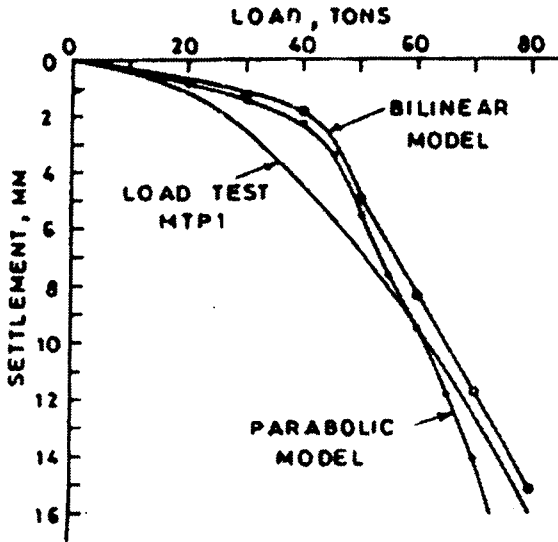


FIGURE 21 : Comparison of Load Test Data at Manali Site (Pile MTP1)

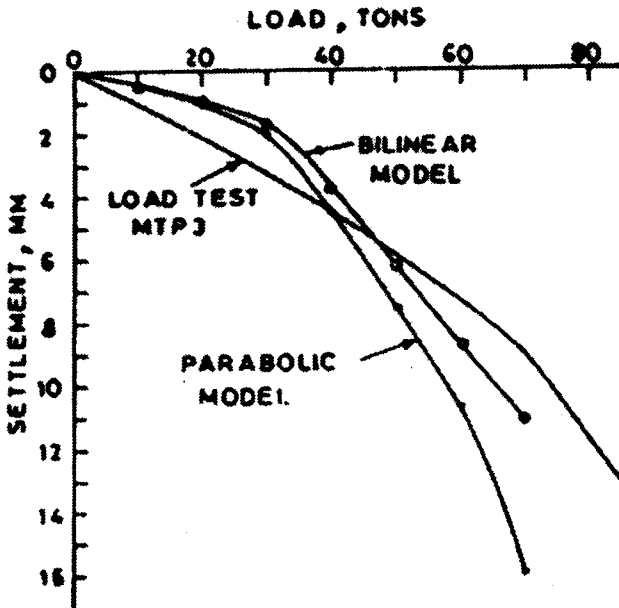


FIGURE 22 : Comparison of Load Test Data at Manali Site (Pile MTP 3)

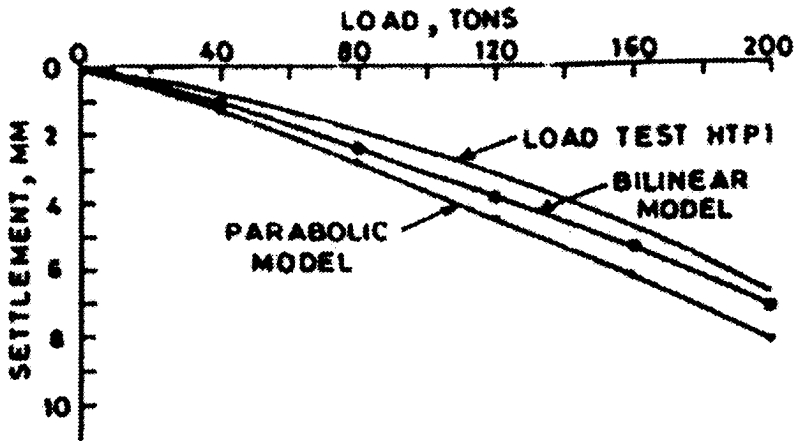


FIGURE 23 : Comparison of Load Test Data at Haldia Site (Pile HTP1)

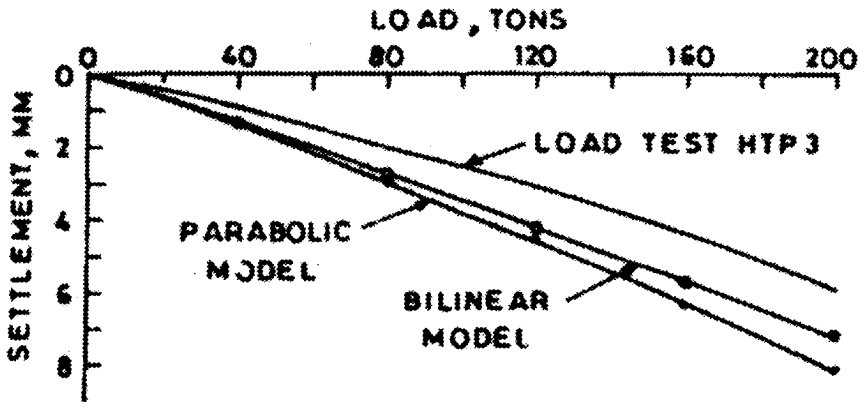


FIGURE 24 : Comparison of Load Test Data at Haldia Site (Pile HTP1)

### Laterally Loaded Piles

Lateral pile load analyses are usually carried out using one of the following procedures (i) based on horizontal subgrade reaction approach (ii) using a non-linear p-y approach which is an extension of the first approach and (iii) assuming the soil to be an elastic continuum. The last mentioned approach has the attribute that soil continuity is taken into account. Semi analytical finite element formulation can be ideally

employed for lateral pile analysis. Randolph (1981) studied the problem of flexible piles under lateral loading and proposed algebraic expressions for pile head displacement and rotation.

*Parametric study on long piles*

In many instances it may be expedient to assume that the modulus of elasticity of soil either remains constant with depth or has a value proportional to depth. For both of these situations the results of the analysis may be conveniently presented using simple dimensionless influence factors (Chandrasekaran et al 1984). Here results of a parametric study for long piles is presented. The effect of variation of Poisson's ratio of the soil is also investigated.

*Homogeneous elastic medium*

Consider a pile as shown in Fig. 25 subjected to a horizontal load  $P_t$  and a moment  $M_t$  embedded in an elastic continuum. When the soil medium is homogeneous it is convenient to define a characteristic length  $T$  given by

$$T = \sqrt[4]{\frac{EI}{E_s}} \tag{13}$$

in which  $EI$  is the flexural rigidity of pile and  $E_s$  is the elastic modulus of the soil.

For given values of  $L/T$ ,  $T/D$  and  $\nu_s$ , and for a particular depth  $x = XT$ , expressions for deflection  $y$ , slope  $\theta$ , bending moment  $M$ , can be written as follows :

$$\left. \begin{aligned} y &= (P_t T^3 / EI) A_y + (M_t T^2 / EI) B_y \\ \theta &= (P_t T^2 / EI) A_s + (M_t T/EI) B_s \\ M &= (P_t T) A_m + M_t B_m \end{aligned} \right\} \tag{14}$$

From a practical point of view values of  $A_y$ ,  $A_s$ ,  $B_y$ ,  $B_s$  at the top of the pile and the variation of  $A_m$  and  $B_m$  with depth are of importance. Table 5 and 6 give the values of  $A_y$ ,  $A_s$ ,  $B_y$  and  $B_s$  for  $L/T = 5$  and  $T/D = 2, 5, 10$  and  $20$  for values of Poisson's ratio equal to  $0.47$  and  $0.1$  respectively. For Poisson's ratio equal to  $0.47$  the variations of influence factors  $A_m$  and  $B_m$  with depth factor  $X$  are presented in Figs. 26 and 27 respectively.

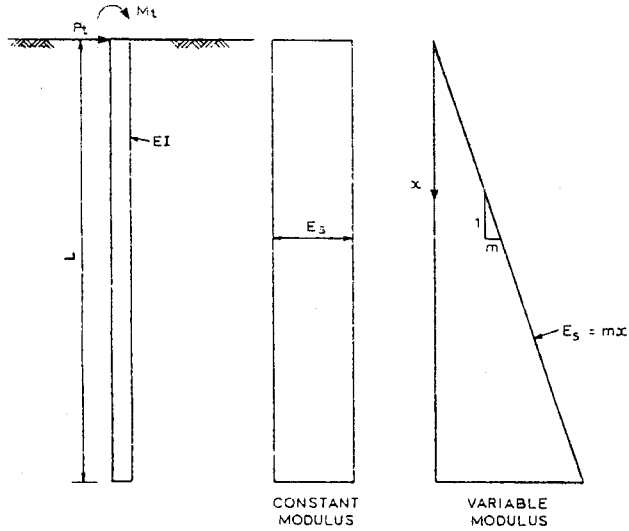


**FIGURE 25 : Soil Modulus Variation Adopted in Parametric Study**

**Table 5. Dimensionless Influence Factors at Pile Head for Piles in a Homogeneous Elastic Medium**

$L/T \geq 5$		$\nu_s = 0.47$		
T/D	$A_y$	$A_s$	$B_y$	$B_s$
2	0.737	- 0.557	0.557	- 0.986
5	1.063	- 0.783	0.783	- 1.230
10	1.262	- 0.897	0.897	- 1.325
20	1.411	- 0.974	0.974	- 1.384

**Table 6. Dimensionless Influence Factors at Pile Head for Piles in a Homogeneous Elastic Medium**

$L/T \geq 5$		$\nu_s = 0.1$		
T/D	$A_y$	$A_s$	$B_y$	$B_s$
2	0.768	- 0.578	0.578	- 0.976
5	1.067	- 0.780	0.780	- 1.220
10	1.258	- 0.886	0.886	- 1.311
20	1.404	- 0.961	0.961	- 1.370

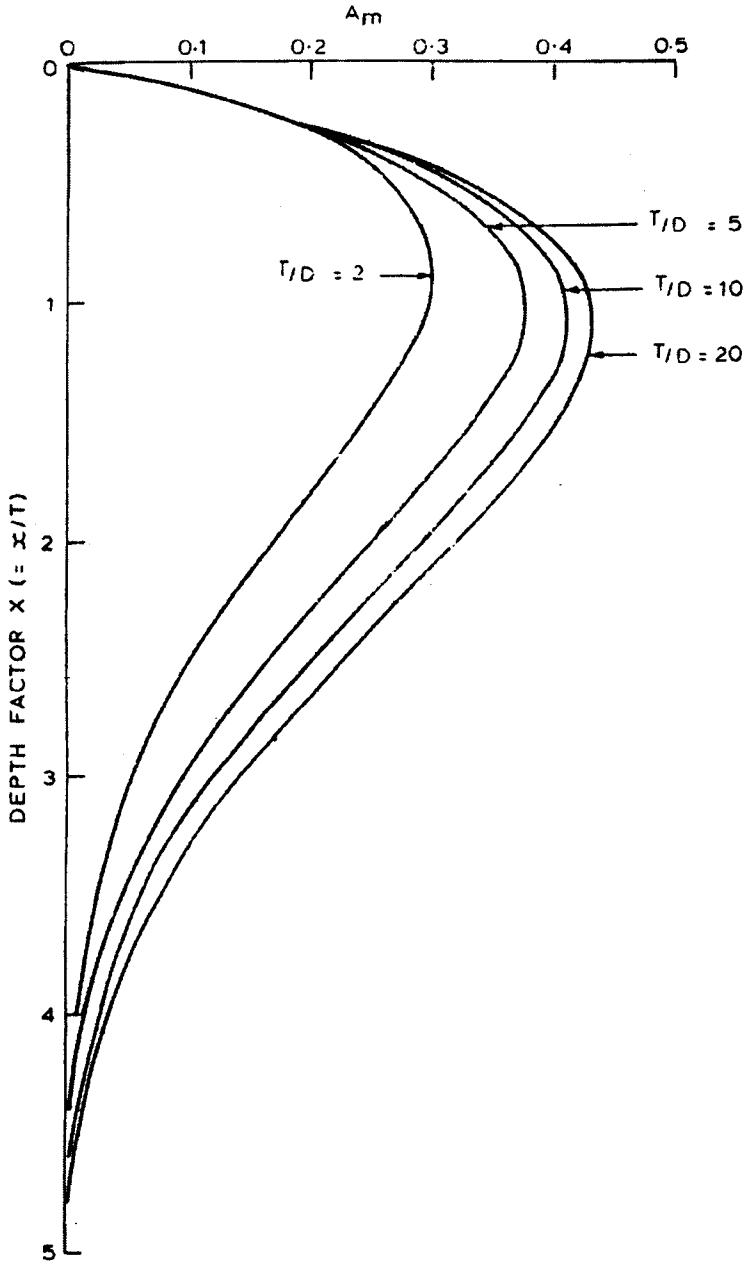


FIGURE 26 : Variation of Dimensional Factor for  $A_m$  with Depth ( $E_s$  Constant)

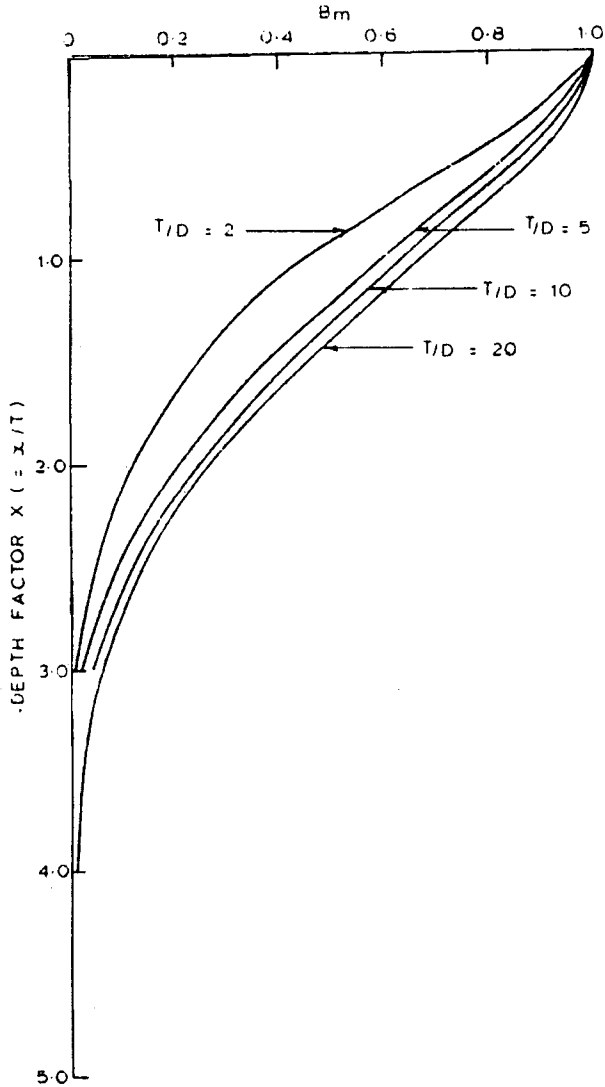


FIGURE 27 : Variation of Dimensionless Factor  $B_m$  for Bending Moment with Depth ( $E_s$  Constant)

### *Inhomogeneous medium*

Consider a soil medium in which the elastic modulus  $E_s$  varies according to the equation  $E_s = mx$  where  $x$  is the depth from the soil surface. For a pile having flexural rigidity  $EI$  embedded in the medium it is convenient to define a characteristic length  $T$ , as

$$T = \sqrt[5]{\frac{EI}{m}} \tag{15}$$

For given values of  $L/T$ ,  $T/D$  and  $v_s$  and for a particular depth  $x = XT$ , expressions for deflection  $y$ , slope  $\theta$ , bending moment  $M$  can again be written by eqs. 14 with  $T$  given by Eq. 15.

Tables 7 and 8 gives the values of  $A_y$ ,  $A_s$ ,  $B_y$  and  $B_s$  at the top of the pile for values of  $T/D = 2, 5, 10$  and  $20$  for Poisson's ratio equal to  $0.47$  and  $0.1$  respectively. For Poisson's ratio equal to  $0.47$  the variation of  $A_m$  and  $B_m$  with depth factor  $X$  are presented in Figs. 28 and 29 respectively. This parametric study indicates that the effect of Poisson's ratio on the behaviour of piles subjected to lateral loads is not significant. For the same flexural rigidity the deflections and bending moments are greater in smaller diameter piles.

**Table 7. Dimensionless Influence Factors at the Pile Head for Piles in Inhomogeneous Elastic Medium with  $E_s = mx$**

$L/T \geq 5$		$v_s = 0.47$		
$T/D$	$A_y$	$A_s$	$B_y$	$B_s$
2	1.285	- 0.974	0.974	-1.254
5	1.804	- 1.289	1.289	-1.541
10	2.099	- 1.441	1.441	-1.636
20	2.310	- 1.543	1.543	-1.695

**Table 8 Dimensionless Influence Factors at the Pile Head for Piles in Inhomogeneous Elastic Medium with  $E_s = mx$**

$L/T \geq 5$		$v_s = 0.1$		
$T/D$	$A_y$	$A_s$	$B_y$	$B_s$
2	1.334	- 0.998	0.998	-1.263
5	1.814	- 1.287	1.287	-1.627
10	2.099	- 1.433	1.433	-1.627
20	2.310	- 1.534	1.534	-1.687

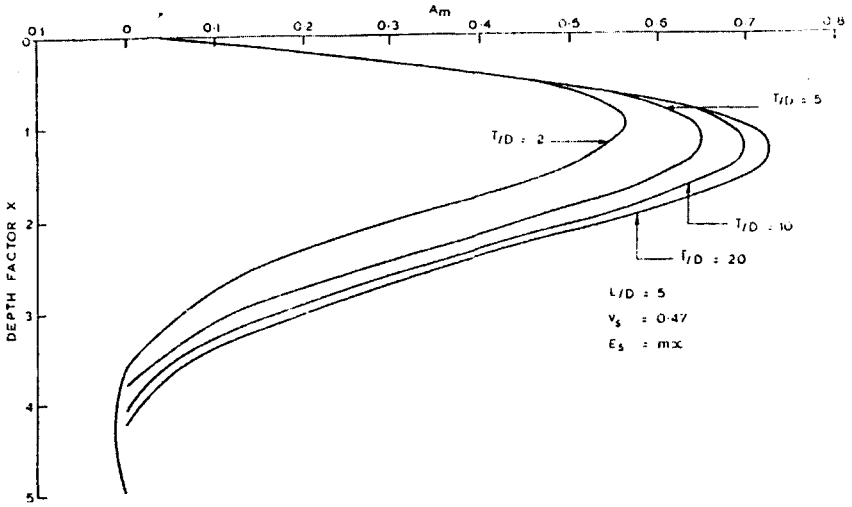


FIGURE 28 : Variation of Dimensionless Factor for Bending Moment  $B_m$  with Depth ( $E_s = \text{max}$ )

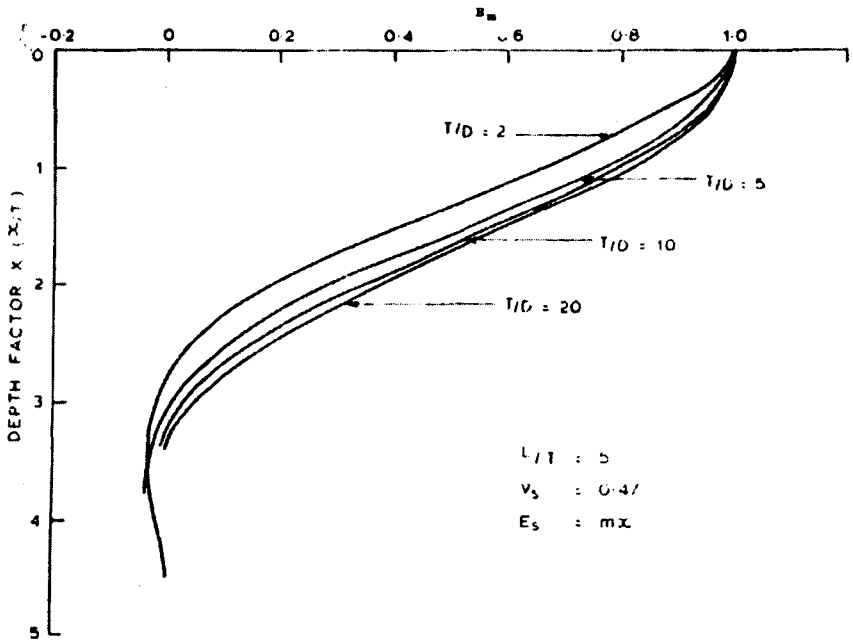


FIGURE 29 : Variation of  $B_m$  with Depth Factor  $X$  for Inhomogeneous Medium

## Part II Centrifuge Modelling

### Introduction

Body force due to gravity plays an important role in geotechnical engineering problems. When studies are undertaken to understand the behaviour of real structures through scaled models, it is found impossible to simulate the body forces in the normal 1g field. Consequently, many phenomena of interest to the geotechnical engineer cannot be reproduced in laboratory models. It has been realised that this deficiency can be overcome with the use of centrifuge technique in which models are subjected to predetermined, high acceleration levels to produce similarity conditions satisfactorily in most situations.

In the international scene, considerable progress has been made in the last two decades years in the utilisation of this technique for a variety of complex problems and the interest of the geotechnical community in this area is reflected by the number of conferences and symposia held on this topic and also by the number of centrifuge facilities built in various parts of the world. Centrifuge modelling is now firmly established as a dependable research tool that can provide solutions to many of the hitherto intractable problems in geotechnical engineering. Some of the important problems relating to earth dams, tunnels, offshore foundations, geo-environmental problems, problems of nuclear waste disposal, seismic studies of earth structures and foundations can be tackled using centrifuge modelling.

### Similitude Relationships

#### *Similar system*

Studies on scaled models are resorted to in engineering disciplines in order to understand the behaviour of the real full-scale structures called prototypes. Here we shall confine ourselves to the subject of physical modelling of geotechnical structures using centrifuges. A physical model involves a real object subjected to forces or displacements and physical quantities such as resulting displacements and stresses are measured. From the physical measurements made on the model, the corresponding quantities are predicted for the prototype. The statement that the physical systems are similar implies not only that they are geometrically similar but signifies much more than this.

Two systems are said to behave similarly when corresponding physical quantities are related by equations of the type

$$R_m = \lambda R_p \tag{16}$$

where  $R_m$  and  $R_p$  are the same physical quantity pertaining to the model and the prototype and  $\lambda$  is the proportionality constant. Different physical quantities may be related by different proportionality constants. The linearity of the relationship is a necessity. It may be emphasised that the relations must be satisfied at geometrically corresponding points throughout the two systems considered at all times subsequent to the initial instant. When two systems behave similarly knowledge of the behaviour of one will enable us to determine what the behaviour of the other must be. Two physically similar systems will behave similarly when certain relevant scale factors are satisfied but not otherwise, in general.

**Modelling of clay slope**

Consider the stability of a clay slope shown in Fig.30 having a slope angle  $i$  under undrained conditions. An estimate of the maximum stable height may be based on the slip circle method of analysis. Based on Taylor's stability chart the maximum stable height of slope  $H_c$  for  $i = 60^\circ$  is given by Eqn. 17.

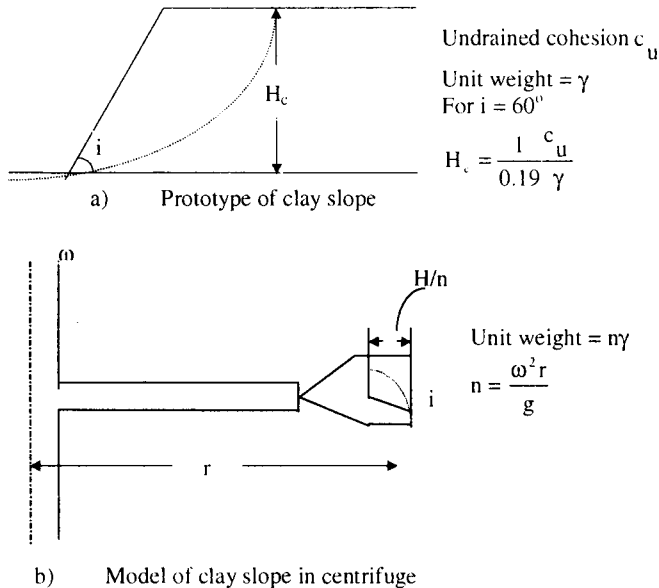


**FIGURE 30 : Centrifuge Modelling of Undrained Behaviour of Clay Slope**

$$H_c = \frac{1}{0.19} \frac{c_u}{\gamma} \quad (17)$$

where  $c_u$  is the undrained cohesion and  $g$  the unit weight of the clay. Suppose if this estimate is to be verified, how could one proceed to carry out a scaled model study by reducing the linear dimension by a factor, say of 50? If experiments are envisaged in 1-g field it becomes necessary to produce a model material having a value of

$$\frac{c_u}{\gamma} = \frac{1}{50} \quad (18)$$

of the value of the prototype material. It is indeed almost impossible to produce a material corresponding to this value of  $c_u/\gamma$ . It is attractive to consider the possibility of increasing the value of  $\gamma$  by placing the model slope in a centrifuge which can increase the unit weight of soil by a factor  $n$ . The method has a lot of other advantages as well, viz. it is not only not necessary to look for a new material but other physical properties such as the stiffness and strength of the material are same which makes the deformations directly scalable.

### *Centrifuge*

Centrifuge is an equipment in which models can be subjected to higher acceleration field. If the model is placed at a radius  $r$  and if the angular velocity is  $\omega$  rad/sec than the radial acceleration is  $\omega^2 r$ . We may visualise this as though the unit weight of the material is increased by a factor  $n = \omega^2 r/g$  where  $g$  is the acceleration due to gravity.

### *Dimensional analysis*

Scaled models in geotechnical engineering seriously lack similitude because stress levels in the model do not match those in the prototype. There are two major factors which need to be considered in modelling of geotechnical structures These are :

- (i) Body force due to gravity which is often the actuating force and
- (ii) Soil properties such as strength and stiffness which are highly stress dependent.

By placing the model in the centrifuge and subjecting it to increased acceleration field it is possible to obtain prototype stress levels in the

models. Centrifuge is a convenient way to provide artificial gravity resulting from centripetal acceleration.

It may not always be possible to satisfy all the similarity laws, the researcher must verify the implications of the departure, It is educative to follow the studies carried out by Ovesen (1980) on the bearing capacity of footings on sand. Let us consider a footing having a diameter  $d$ , resting on dense homogenous sand and subjected to a bearing pressure  $p$ . Let the vertical settlement of the footing be  $s$ . How could one set up a model experiment, to obtain the values of  $p$  and  $s$  till failure? The following eight independent physical quantities might influence the behaviour:

$\gamma$	(N/m <sup>3</sup> )	unit weight of the sand
$d$	(m)	diameter of the footing
$e$	(-)	void ratio of the sand
$\phi_\mu$	(-)	angle of inter-particle friction between sand grains
$\sigma_c$	(N/m <sup>2</sup> )	inter-particle cohesion between sand grains
$\sigma_g$	(N/m <sup>2</sup> )	crushing strength of the grain material
$E_g$	(N/m <sup>2</sup> )	modulus of elasticity of grains
$d_g$	(m)	average grain size

Two basic units namely length and force are involved in the above quantities. Let us choose  $d$  and  $\gamma d$  to represent the above units. In dimensional analysis a well known theorem called PI theorem due to Buckingham is used. Simply stated, if there are  $n$  quantities governing a physical phenomenon and there are  $m$  dimensions involved, then  $(n-m)$  independent dimensionless factors could be found which govern the phenomenon. Further, each of these factors could be represented as a function of the remaining factors. In this case for a given  $s/d$  we may write

$$\frac{p}{\gamma d} = f \left( e, \phi_\mu, \frac{\sigma_c}{\gamma d}, \frac{\sigma_g}{\gamma d}, \frac{E_g}{\gamma d}, \frac{d_g}{d} \right) \quad (19)$$

For complete similarity all the six dimensionless factors must attain the same values in the model and the prototype. The model and prototype are then said to be similar. While ideally complete similarity is desirable in a model study, it is indeed difficult to meet all the requirements. It is the job of the experimenter to so design the experiment that all the

major factors are correctly modelled and if there are any deviations, their influence is negligible. Further, the experimenter should satisfy himself this is really so.

**Tests in 1g field**

Let the diameter of the footing be reduced by a factor n. The soil used is the same as in the prototype. The comparison between prototype and model values of the dimensionless factors identified earlier is shown in Table 9. It is clearly seen that similitude criteria are violated with respect to four factors.

**Test carried out in a centrifuge**

The diameter of the footing is reduced by a factor n and the same soil as the prototype is used in the experiment. Now the test is carried out in a centrifuge where the model is subjected to an acceleration equal to ng increasing the body force to a value nγ. Table 9 shows how the similarity relations in a centrifuge are satisfied. Out of six factors five are matching and only one is not matching. The experiments carried out

**Table 9. Similitude Comparison**

	Prototype scale 1/1, gravity g	Conventional model scale 1/n, gravity g		Centrifuge model scale 1/n, gravity ng	
1.	e	e	similar	e	similar
2.	θμ	θμ	similar	θμ	similar
3.	$\frac{\sigma_c}{\gamma_d}$	$\frac{\sigma_c}{\gamma} \frac{d}{n}$	not similar	$\frac{\sigma_c}{\gamma_n} \frac{d}{n}$	similar
4.	$\frac{\sigma_g}{\gamma_d}$	$\frac{\sigma_g}{\gamma} \frac{d}{n}$	not similar	$\frac{\sigma_g}{\gamma_n} \frac{d}{n}$	similar
5.	$\frac{E_g}{\gamma_d}$	$\frac{E_g}{\gamma} \frac{d}{n}$	not similar	$\frac{E_s}{\gamma_n} \frac{d}{n}$	similar
6.	$\frac{d_g}{d}$	$\frac{d_g}{d_n}$	not similar	$\frac{d_g}{d_n}$	not similar

by Ovesen (1980) with different footing sizes at different values of  $N$  modelling the same prototype confirmed the efficacy of centrifuge modelling. Further Ovesen's experiments indicated that the ratio of diameter to average grain size of less than 15 introduced minor scale effect. Whatever may be the scaling relations they must be verified by experimental results. They could be in the form of direct comparison between prototype and centrifuge experiments or between centrifuge model tests at various scales the latter method of comparison is called modelling of models.

### ***Scaling laws***

In the centrifuge the linear dimensions are modelled by factor  $1/n$  and the stress is modelled by a factor of unity, We may work out the various scaling relationships based on these two factors. For example

$$L_m = L_p / n \text{ and } \sigma_m = \sigma_p \quad (20)$$

$$\begin{aligned} \text{force} &= \text{stress} \times \text{area} \\ F_m &= 1 \times (1/n^2) F_p = (1/n^2) F_p \end{aligned} \quad (21)$$

$$\begin{aligned} \text{energy} &= \text{force} \times \text{distance} \\ E_m &= (1/n^2) (1/n) \times E_p = (1/n^3) E_p \end{aligned} \quad (22)$$

Similarly other relations between model and prototype may be worked out. For diffusion problems the differential equation governing the process will have to be used to establish the relationship for time between model and prototype. This relationship is different from the one for inertia. Different strategies will have to be adopted when inertia effects and diffusion effects are to be simultaneously considered. Various commonly used scaling relations are shown in Table 10.

### **Errors in Centrifuge Experiments**

Although centrifuge simulates prototype conditions in a scaled model there are a few errors whose effects should be kept to a minimum.

#### ***Error due to model material***

A question which is often posed is with respect to the validity of using the prototype material to construct the model. If the footings and piles are scaled down by a factor  $n$  they would then interact with far lesser number of soil particles and the results may deviate from the

**Table 10. Scaling Laws**

Quantity	Prototype	Model
Length	n	1
Area	n <sup>2</sup>	1
Volume	n <sup>3</sup>	1
Velocity	1	1
Acceleration	1	n
Mass	n <sup>3</sup>	1
Force	n <sup>2</sup>	1
Energy	n <sup>3</sup>	1
Stress	1	1
Strain	1	1
Mass density	1	1
Energy density	1	1
Time (dynamic)	n	1
Time (diffusion)	n <sup>2</sup>	1
Time (creep)	1	1
Frequency	1	n

scaling relations which are based on continuum assumptions. Tests based on modelling of models concept (Ovesen 1980) will allow detection of any departure and provide guidelines regarding the limitations of scaling concepts arising from grain size effects. This effect has been studied in detail by several investigators and by adopting suitable size models, the errors due to this can be made insignificant.

***Errors due to varying acceleration field***

Another source of error is the error due to varying acceleration field in the model. In the centrifuge each point in the model is subjected to a body force field which is directed radially outwards and has a magnitude equal to  $\rho\omega^2r$ . Consider a soil bed modelled in the centrifuge between radii  $r_1$  and  $r_2$  as shown in Fig.31. The vertical stress at radius  $r$  in the model will be

$$\sigma = \gamma\omega^2 \int_{r_1}^r r dr = \frac{\gamma\omega^2}{2} (r^2 - r_1^2) \tag{23}$$

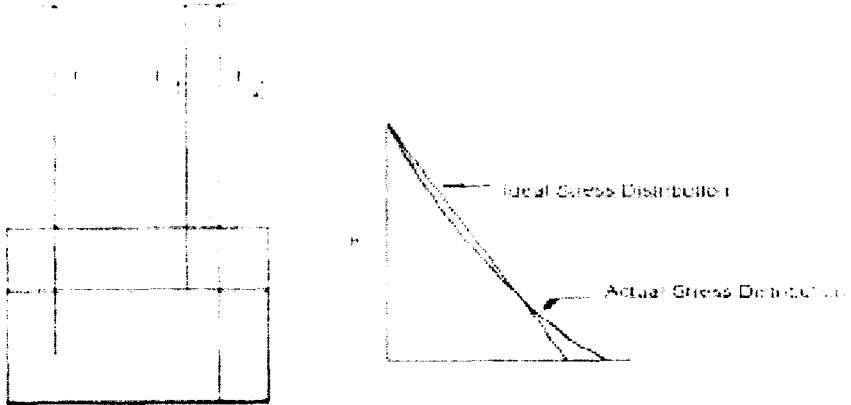


**FIGURE 31 : Vertical Stress due to Varying Acceleration Field in Centrifuge**

There is thus a deviation from the desired linear variation of the vertical stress with depth and the stresses in the model will not match with the filed stress precisely (see Fig.31). They match at the top where  $r = r_1$  and can be matched at one other position  $r = r_0$ . By keeping the maximum understress and overstress errors to be equal a nominal radius  $r_0$  can be worked out as

$$r_0 = r_1 + \frac{2}{3}(r_2 - r_1) \quad (24)$$

### ***Error due to extra-tangential acceleration***

This error stems from extra-tangential acceleration in a model which arises from the fact that the acceleration field is distributed radially in the rotating plane of the arm (see Fig.32). This error is related to the semi-width of the model at a given radius  $R'$ . Its value is equal to  $1/R'$  times the radial acceleration at  $R'$ . This error occurs only in horizontal plane or the plane of rotation. In vertical plane this error is not present. This error takes the form of horizontal component of acceleration field. Due to this error there can be a variation in actuating forces in the model resulting in reduced or increased deformations and delayed or premature failure depending upon the position of model.

This error can be reduced by increasing the radius, but the cost of the facility will rise significantly due to this. This error can also be reduced by placing the model close to the centreline of the strong box, but this may not always be feasible.

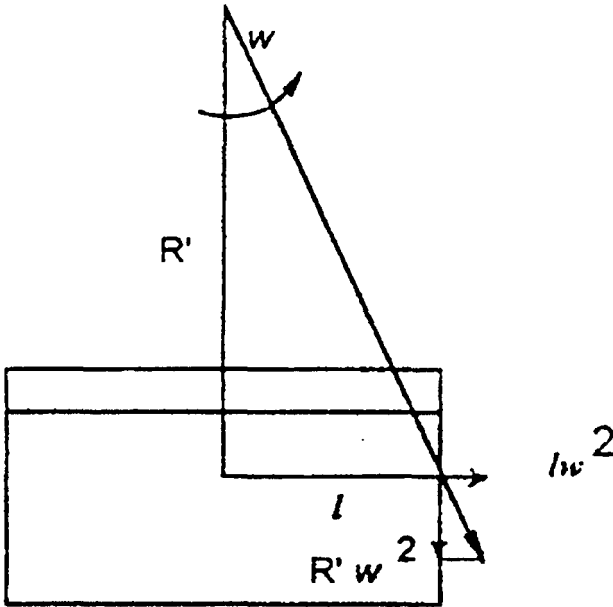


FIGURE 32 : Error due to Extra Tangential Acceleration

In two dimensional problems such as dams, embankment or tunnels, this error can be eliminated in the lateral plane by placing the model such that its longitudinal dimension is in the plane of rotation. By such placement the extra-tangential error occurs in the longitudinal direction of model and do not affect much the stress conditions in lateral direction. Using varying acceleration field in finite element analyses error due to extra-tangential acceleration has been studied by Chandrasekaran and Gadre (1994) for the problem of vertical cuts.

***Errors due to Coriolis force***

In the plane of rotation the model experiences what is known as Coriolis acceleration given by

$$a_c = 2 \omega \times v \tag{25}$$

where  $a_c$  = Coriolis acceleration;  $\omega$  = angular velocity of the centrifuge;  $v$  = velocity of the soil relative to the strong box.

This acceleration field in the centrifuge is given by

$$a = \omega^2 R_c = \omega V \tag{26}$$

$R_e$  = effective model radius

$V$  = velocity of model during rotation

For  $a_c / a$  to be less than ten percent implies that  $v$  be less than 0.05  $V$ . This perhaps may be considered as an upper limit for slow events (Taylor 1995).

## **Present Status**

Many countries have installed large centrifuge facilities devoted to geotechnical studies. They include U.K., Japan, France, USA, Russia, West Germany, Netherlands, Denmark, Australia, Canada, Italy and China. A wide range of problems are now being tackled using these facilities. The following are some of the areas which are currently being studied in different centrifuge installations.

### *Soil structure interaction*

foundations of buildings

mat foundations

deep foundations

pile foundations

retaining structures, tie back systems, slurry walls

reinforced earth, geotextiles, geogrids and geomembranes

buried conduits, culverts, underground structures

tunnels, lined tunnels

shafts, lined shafts

### *Dams and embankments*

earth dams, interaction with abutments, differential settlement, stability in overtopping, sudden drawdown

levees on soft ground, defences along major rivers, long term stability

gravity dams, foundations interaction mine waste tailings

### *offshore structures*

piles, anchors, cyclic loading

foundations of jack-up rigs

gravity structure foundations, liquefaction

submarine slopes

interaction of mud movements with structures

### *Geophysical structures*

geological structures  
nuclear waste disposal  
hydrofracture

### *Environmental geotechniques*

contaminant transport  
performance of liners

### *Blast effects*

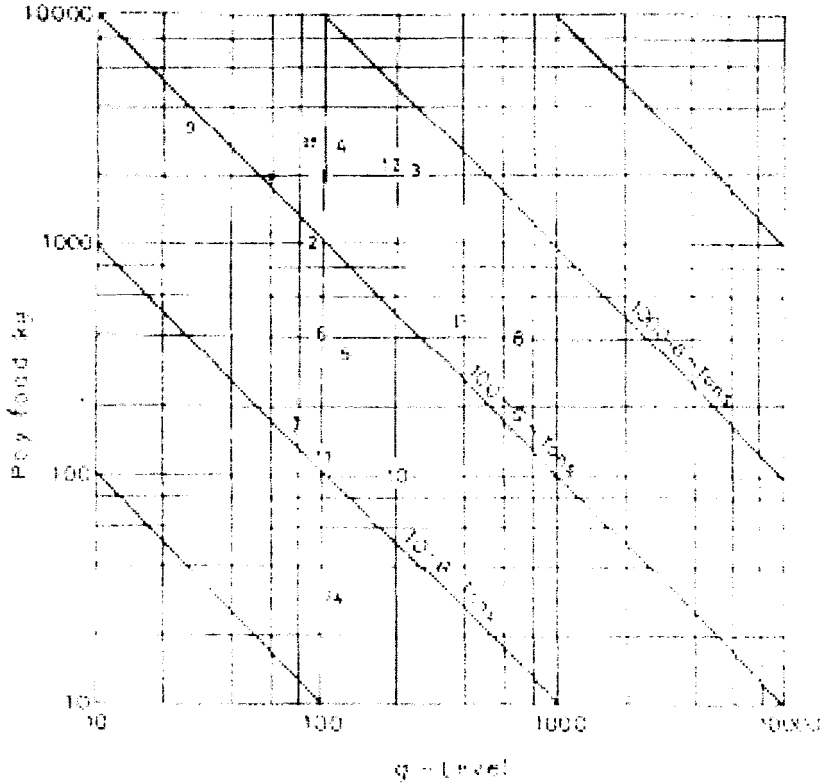
cratering  
block caving  
containment  
subsidence  
liquefaction

### *Earthquake and vibration*

dam safety  
nuclear power plants  
dynamic soil structure interaction  
liquefaction  
machine foundation  
wave forces  
fault movement

### *Centrifuge capacities*

There are a number of parameters which are important from the point of view of centrifuge usefulness. They include the maximum payload, the maximum acceleration achievable, the nominal radius and the dimensions of the soil model that could be placed in the bucket. One way of classifying the centrifuge capacities is in terms of g-tons which is calculated as the maximum value of the product of the acceleration in g's and the payload in tons. The payload *versus* g may be shown in a log-log plot. In such a diagram centrifuge with the same g-ton capacity will be shown to fall on the same line down the right of the chart. Fig. 33 shows the capacity of some of the existing installations.



- |                            |                       |
|----------------------------|-----------------------|
| 1. LCPC, France            | 9. Davis, I Stage     |
| 2. Cambridge, U.K.         | 10. Tyndal, U.S.A.    |
| 3. Bachum, West Germany    | 11. Colorado, U.S.A.  |
| 4. Port and Harbour, Japan | 12. Colorado, U.S.A.  |
| 5. Public Works, Japan     | 13. Wuhan, China      |
| 6. City University, U.K.   | 14. Caltech, U.S.A    |
| 7. Liverpool, U.K.         | 15. IIT Bombay, India |
| 8. Bergamo, Italy          |                       |

FIGURE 33 Capacities of Centrifuges

## Experience with Small Geotechnical Centrifuge at IIT Bombay

A small geotechnical centrifuge was fabricated and installed in IIT Bombay in 1992 with the following specifications.

Maximum payload	: 2.4 kg
Arm radius	: 33 cm
Maximum acceleration	: 300 g
Strong box internal dimensions	: 9 x 10 x 8 cm
Instrumentation	: Stroboscope and window electrical and hydraulic slip rings, on-board 4 channel data logger
Parameters measured	: Displacement

Fig.34 and Plates 1 and 2 show this facility. This facility is admittedly small. However ever since it became available a large number of studies have been completed using even this small facility. The studies included

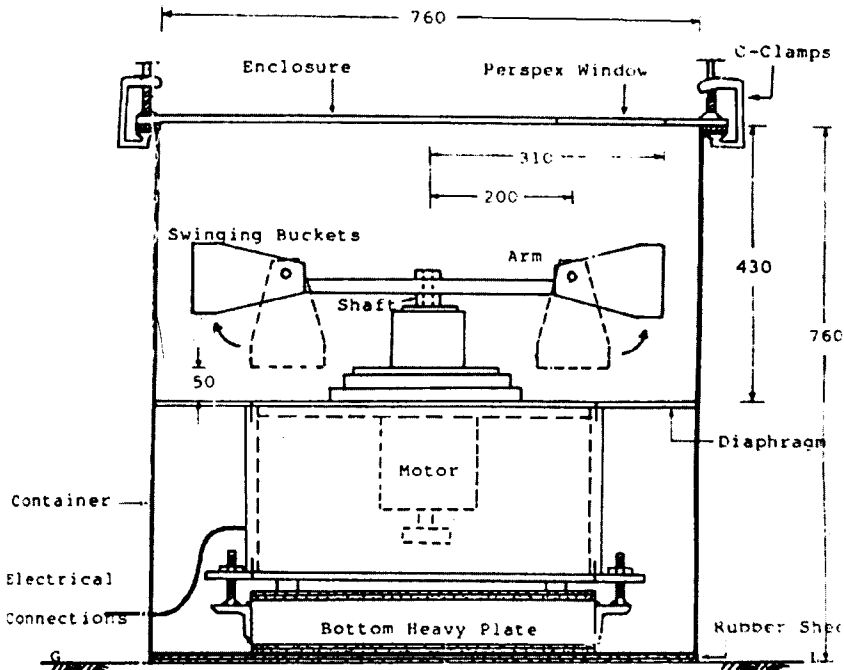
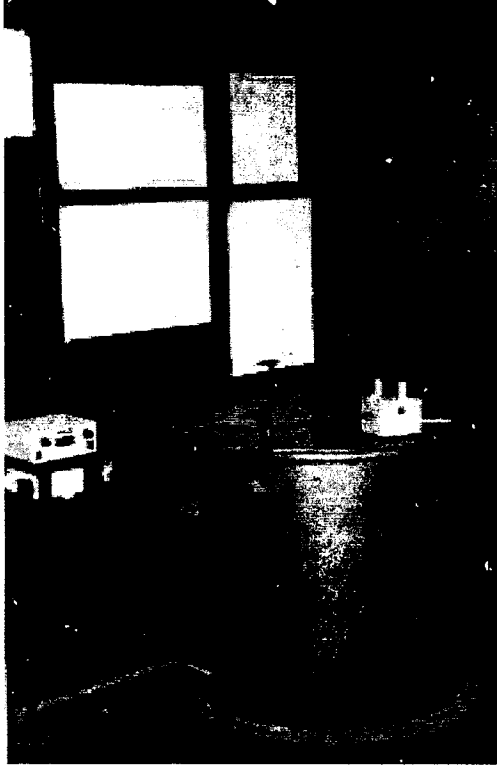
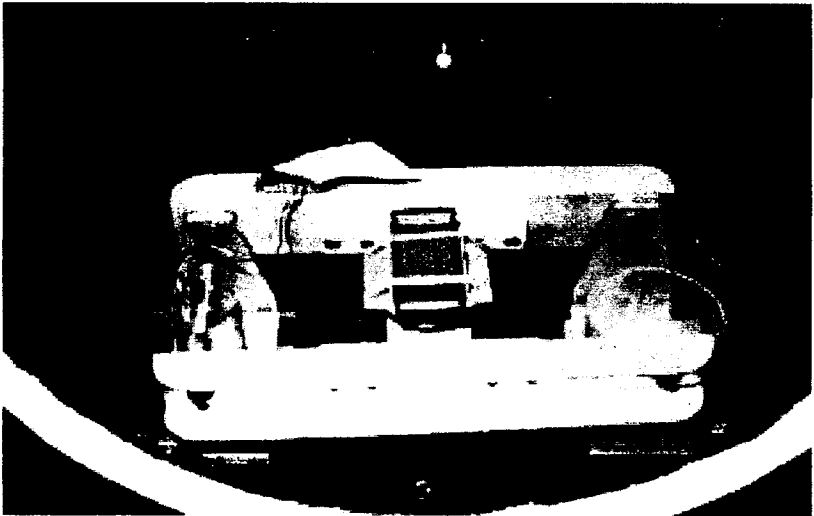


FIGURE 34 : Small Geotechnical Centrifuge



**Plate 1. Overall View of Small Geotechnical Centrifuge**



**Plate 2. Inside View of Small Geotechnical Centrifuge**

Stability of slopes  
 Stability of vertical cuts  
 Stability of fly-ash slopes  
 Reinforced slopes  
 Stability of rainfall induced slope  
 Self weight consolidation  
 Studies on tunnels  
 Settlement of tanks on clay medium  
 Studies on laterally loaded caisson  
 Performance of stone column foundations  
 Reinforced earth retaining walls Stability of shallow foundation

This simple facility has generated considerable enthusiasm amongst the students and faculty. The facility has been used in 25 Masters and 2 Ph.D theses.

Some of the simple experiments carried out in the small geotechnical centrifuge are described here for the purpose of illustrating usefulness of the equipment.

### ***Experiments on circular tunnel***

The experiment was carried out with soil having a  $c_u = 41.2 \text{ kN/m}^2$  and  $\gamma = 19.3 \text{ kN/m}^3$ . The diameter of the tunnel was 2 cm in the model simulating a prototype of 6m diameter at 300g or 962rpm and 6.5m diameter at 1000rpm. There was noticeable change in diameter at 800 rpm. The top portion of the grid was distorted slightly. Since no crack was observed the speed was increased to 1000 rpm when diagonal cracks were observed. The final diameter of the tunnel was 1.5cm. Fig.35 shows the grid before and after testing. Plates 3 and 4 show the model before and after the test. The pattern of cracks and mass flow was similar to the one usually observed in practice.

### ***Stability of clay slope***

A  $60^\circ$  model slope of clay having  $c_u = 51.45 \text{ kN/m}^2$ , and  $\gamma = 18.82 \text{ kN/m}^3$  was tested in the centrifuge. The height of the slope was 6.5cm. A failure surface was noticed to develop at 847 rpm corresponding to 215g. The prototype height of failed slope was may be calculated as 13.98m. For the above material the critical height using Taylor's stability number is  $5.25 \times 51.45 / 18.82 = 14.35\text{m}$ . The experimental and

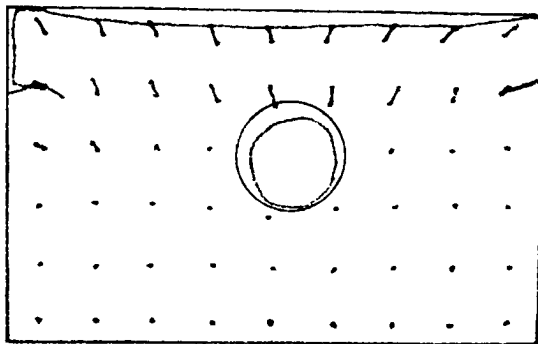


FIGURE 35 : Tunnel Deformation in Centrifuge Experiment

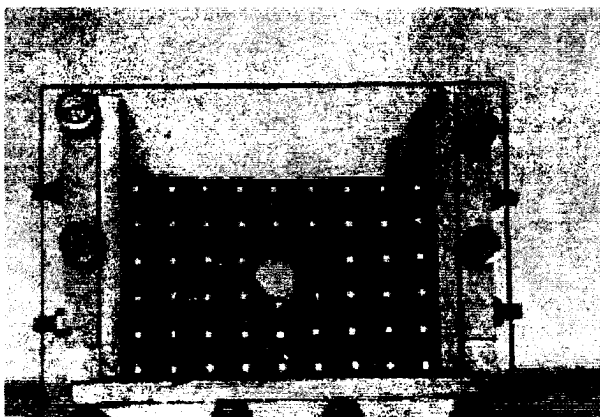


Plate 3. Circular Tunnel in Clay Before Test

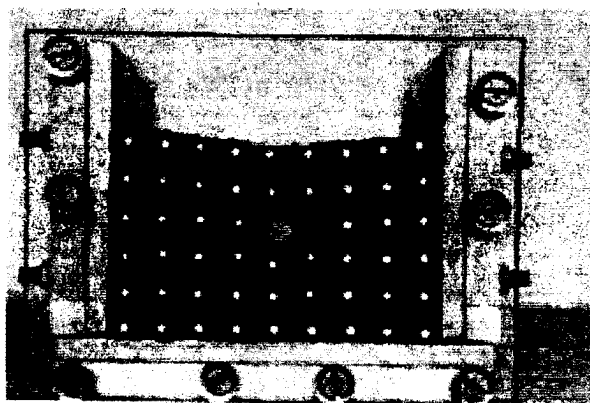


Plate 4. Deformation of Circular Tunnel in Clay after the Test

theoretical values of  $H_c$  show remarkable agreement. The Fig.36 shows the failure pattern as observed from the centrifuge test.

### *Vertical trench*

The vertical model trench of height 4.8cm and width 2m made of clay having  $c_u = 40.8 \text{ kN/m}^2$  and  $\gamma = 18.33 \text{ kN/m}^3$  was expected to fail at 744.3 rpm. (178.44g) corresponding to a critical height of 8.565m. The left side failed at 770 rpm (19.965g) and the right side failed at 785 rpm (198.475). Plates 5 and 6 show the trench before and after failure.

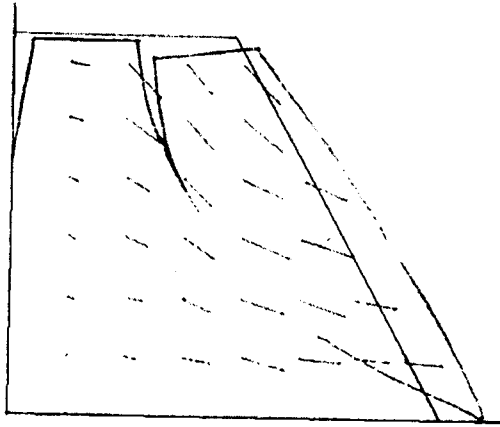


FIGURE 36 : Failure of slope in Centrifuge

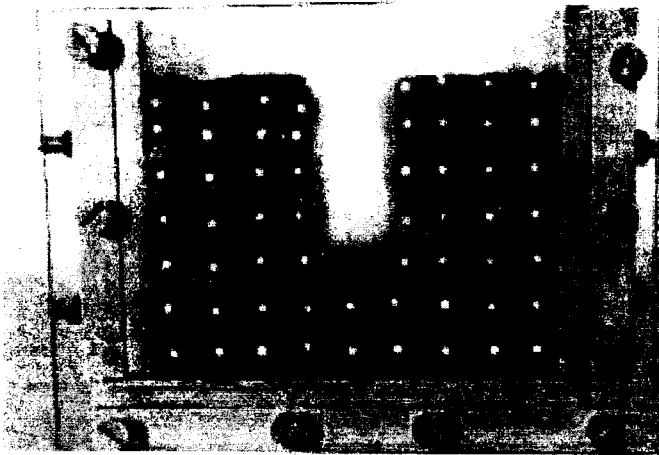


Plate 5. Trench Before Test

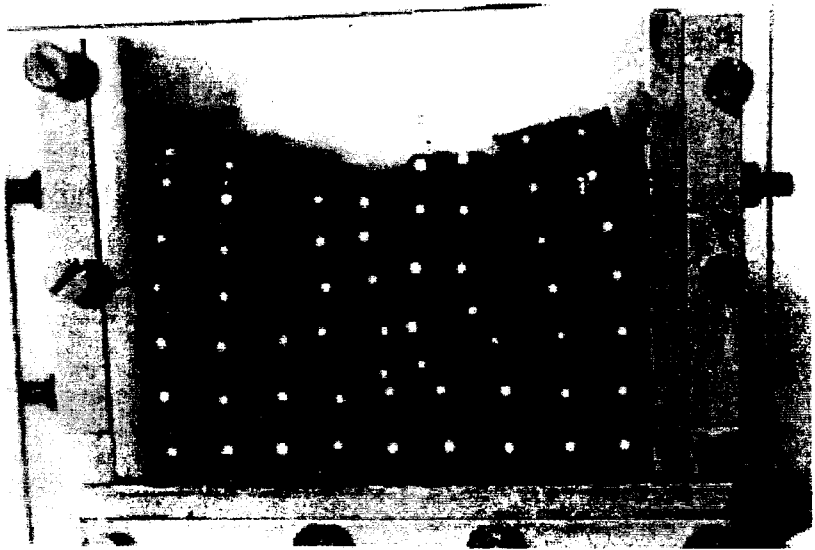


Plate 6. Trench After Test

## Centrifugal Model Studies on Laterally Loaded Pile Groups in Sand

In foundation engineering practice, piles are frequently used to resist large, horizontal loads from the superstructure. They are quite often installed in groups of several piles at fairly close spacings. Extensive literature is available on the laboratory and field performance of laterally loaded single piles and some methods based on certain simplifying assumptions have been proposed for their analysis and design (Reese and Matlock, 1956, Banerjee and Davies, 1978 and Poulos, 1971).

O'Neil and Ghazzaly (1977) proposed a method based on  $p$ - $y$  relationships, but introducing group interaction factors computed by means of the Mindlin's solution. Poulos (1971) made use of the integral equation method modelling the soil as an elastic continuum. Randolph (1981) presented simplified algebraic expressions for the purposes of design. It is recognised that these methods of analysis do not adequately reflect the actual mechanism by which the load transfer takes place within the soil medium and among the individual piles of the group. Thus in order to evolve a satisfactory method of analysis, it is necessary to obtain for comparison results, of laboratory model tests or full-scale field tests on laterally loaded pile groups. Here the results of centrifuge tests on pile groups in sand are described (Kulkarni et al. 1985)

The experiments were carried out in the centrifuge in the soil mechanics laboratory of the University of Liverpool. Details of the centrifuge are available elsewhere (King, et al. 1984). The soil used in the experiments was dry sand, fine grained and uniform. It had an effective size of 150 microns and a uniformity coefficient of 1.5. The unit weight of sand as compacted was  $16 \text{ kN/m}^3$ .

Considering the size of the centrifuge bucket and the instrumentation requirements, the model piles selected were of 24.5872 mm OD, 0.3048 mm wall thickness and 330 mm length (of which the embedded length was 180mm). The material of the piles was 304-SS grade stainless steel with the Young's modulus value of  $1.9284 \times 10^8 \text{ kN/m}^2$ .

Two and three piles groups at two and three diameter spacings (2D and 3D) between centres and rigidly connected to an aluminium cap, 12.5 mm thick, were used in the experiments. The general arrangement of the set-up is shown in Fig. 37 and the load configurations in Fig. 38. Repeat tests were carried out in all cases to ensure fair reproducibility in the data obtained.

Two piles were instrumented, one with 12 pairs and the other, with six pairs of strain gauges, fixed internally in the tubular section. Lateral load was applied to the pile cap through a cable pulled by a gear box-

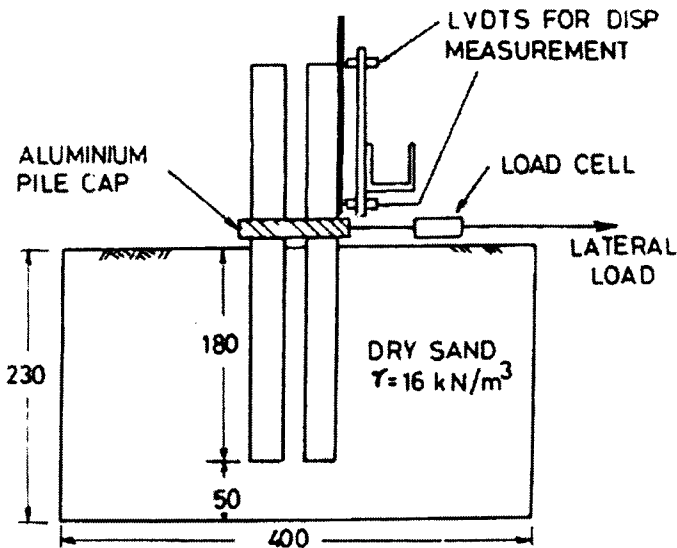
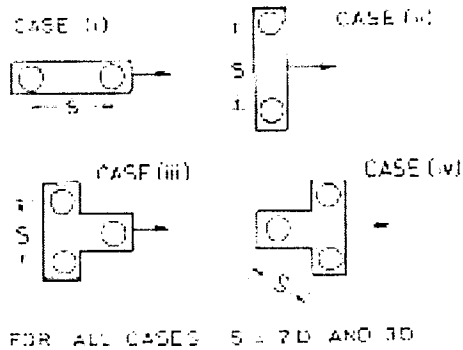


FIGURE 37 : Experimental set-up of Lateral Pile Load Test



**FIGURE 38 : Group and Load Configuration**

motor unit which was operated externally through slip rings. The applied load was measured by means of a load cell and the pile cap deflection and rotation measured through two displacement transducers. Lateral load was applied in suitable increments until the pile head deflections reached values of about 10 per cent pile diameter, i.e. about 2.5mm. The model pile used in this investigation represents a prototype steel pile of 1.23 m diameter and 15.2 mm thickness embedded in sand to a depth of 9m below the ground level. All experimental results are presented for the prototype.

### *Single pile test*

The deflection at ground level and rotation at head are shown in Fig.39. The load deflection curve exhibits an initial linear variation up to a deflection of 5 to 10mm (that is, up to about 0.4 to 0.8 per cent pile diameter), then a curvilinear portion up to about 50mm deflection (corresponding to nearly 4 per cent pile diameter) and a third segment which continues to be linear even up to 120mm deflection (about 10 per cent pile diameter). The pile itself showed no signs of permanent deformation.

By back-analysis the rate of increase of horizontal subgrade reaction  $n_h$  was determined by matching the deflections at levels corresponding to one-half and one percent of pile diameter with the aid of coefficients developed by Reese and Matlock (1956). The corresponding  $n_h$  values worked out to 25676 kN/m<sup>3</sup> and 19929 kN/m<sup>3</sup>. The pile length to characteristic length ratio  $L/T$  at these deflections were 3.73 and 3.55 respectively. It may be noted that these values are only slightly smaller

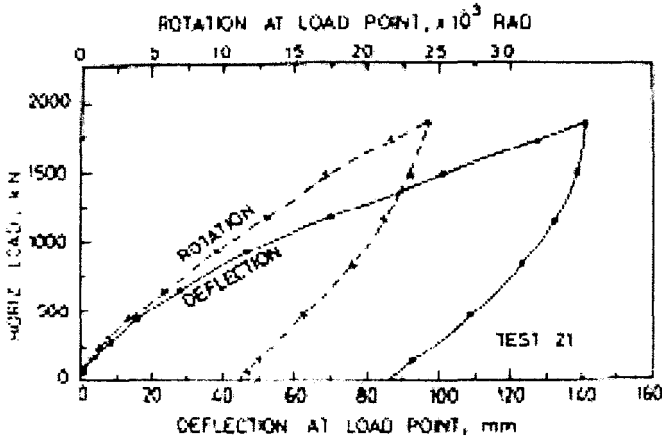


FIGURE 39 : Pile Head Displacement : Single Pile

than the lower limit for long, flexible piles. The results were also back-analysed using the half-space model in which the elastic modulus is proportional to depth. The proportionality constant  $m^*$  for shear modulus, as defined by Randolph (1981), was found to have values of  $4474 \text{ kN/m}^3$  and  $3525 \text{ kN/m}^3$  for one-half and one percent deflections at ground level respectively.

It may be seen that even within the small deflection range of one percent, there is a large variation in the soil parameters  $n_h$  and  $m^*$ . This indicated that linear theories have only limited applicability in the prediction of pile deflections.

The bending moment distributions along the pile length computed by both the approaches are shown in Fig.40 along with the experimental values. Both the distributions agree reasonably well with the observed values in the upper half of the pile, while there is some difference in the lower half. The estimates of maximum bending moment and the corresponding depths are also in close agreement with the experiment.

The above analysis shows that the choice of soil parameters is of crucial importance for prediction of pile behaviour. In this respect, the subgrade reaction theory is less helpful for design purposes, since the  $n_h$  parameter is not unambiguously related to any basic soil properties.

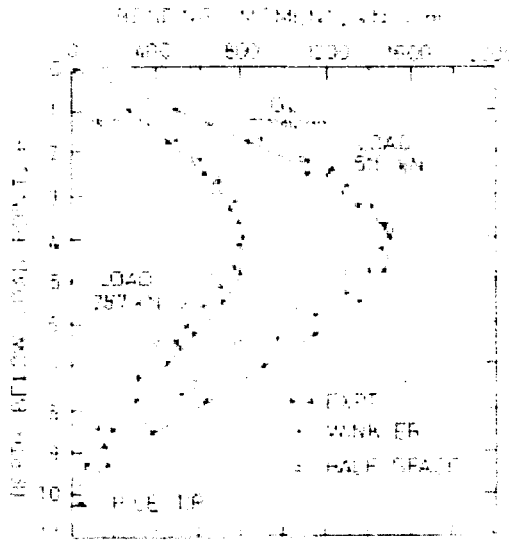


FIGURE 40 : Comparison of Bending Moments for a Single Pile

*Two-pile groups*

The results of two-pile groups are shown in Fig.41. When the pile groups are subjected to horizontal loads in a direction normal to the line joining the pile centres (case ii), a closer spacing of 2D is seen to make little difference compared to 3D spacing. Nevertheless the group load is less than that carried by two single piles. The difference, however, is

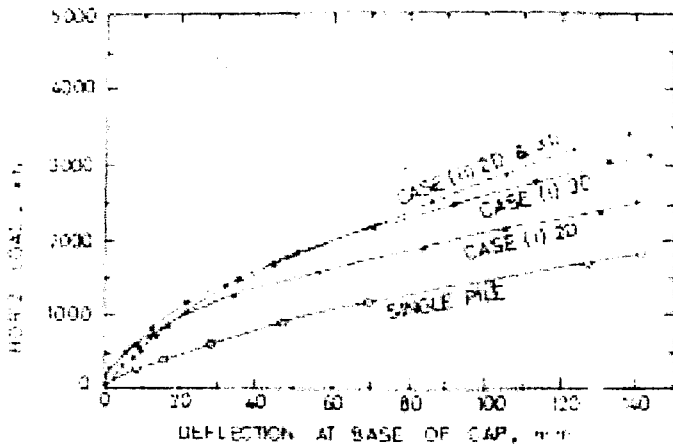


FIGURE 41 : Comparison of Two-pile Groups

small indicating a low level of interaction between adjoining piles. Computations based on the elastic continuum model, using the  $m^*$  parameter determined for the single pile at one percent deflection and using Randolph's (1981) interaction factors for this configuration, give loads of 669 kN for 2D spacing and 699 kN for 3D spacing. The corresponding observed values for both spacings was about 600 kN. Thus even at one percent deflection, the computations tend to overestimate the lateral load.

When lateral loads are applied along the line joining the pile centres in a two-pile group (case i), the group behaviour is influenced by a combination of three effects, viz. the interaction between piles through the soil medium; the axial push-pull effect which would increase the group rigidity depending upon the pile spacing in the configuration; and the type of restraint that develops between the cap and the individual piles.

The results indicate that, in general, for this configuration the load carried by the group at a given deflection is less than twice the corresponding single pile loads. However, at 3D spacing, the load per pile at a given deflection is larger than at 2D spacing.

Estimates of lateral load for one percent deflection were made on the basis of the continuum model using the interaction factors and the  $m^*$  parameters determined for the single pile. At 2D spacing, the load required was found to be 915 kN, compared to the observed value of 750 kN. For 3D spacing, the computed and measured lateral loads were 1238 kN and 850 kN respectively. The consistently lower experimental values of loads compared to the calculated ones indicate that even at very small deflections, the elasticity theory is inadequate, inasmuch as it does not account for the plastic flow of the soil behind and around the front pile and the consequently diminished reaction on the rear pile.

It may be noted from Fig.42 that the front pile experiences a much larger bending moment than the rear pile to the extent of about 100 to 120 per cent. The elastic continuum model, however, envisages equal sharing of the horizontal load among the individual piles and consequently leads to an underestimate of the flexural stress.

The observed slopes of the bending moment curves at the level of the base of the cap indicate that the front pile sustains a greater share of the of the applied load. This should be expected in view of the greater soil resistance likely to be encountered by the front pile. The restraining

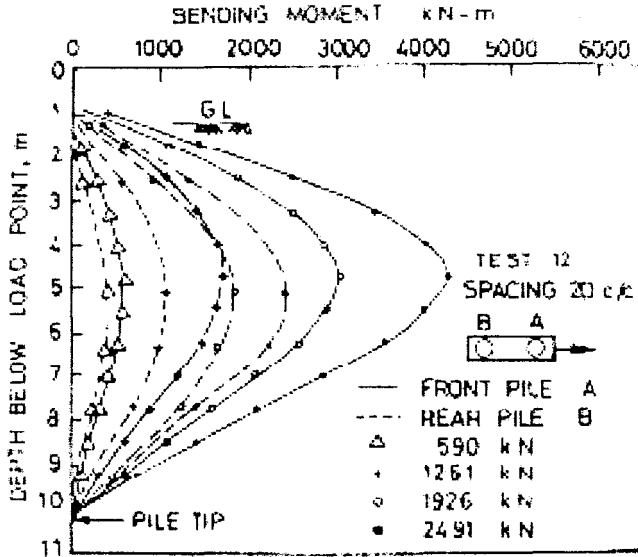


FIGURE 42 : Bending Moments in two-pile Groups

moments at the cap level are also observed to be larger for the front pile.

### *Three-pile groups*

The experimental results for three pile groups are shown in Fig.43. It may be seen that at 2D spacing both the load cases (iii) and (iv) have produced nearly identical load-deflection behaviour. The loading direction appears less relevant at this close spacing. At 3D spacing, the two front piles in case (iv) together mobilise a much higher soil resistance than the load case (iii). It was observed that the maximum bending moments in the front and rear piles are nearly equal and they also occur at about the same depths. This does not, however imply equal sharing of horizontal load among the piles, since the slopes of the bending moment curves, that is, the shear, at the level of the base of the cap are significantly different for the front and rear piles. This observation emphasizes the fact that the rear piles experience a much lower level of soil resistance at nearly all stages of loading a fact not considered in the elastic theories currently in use.

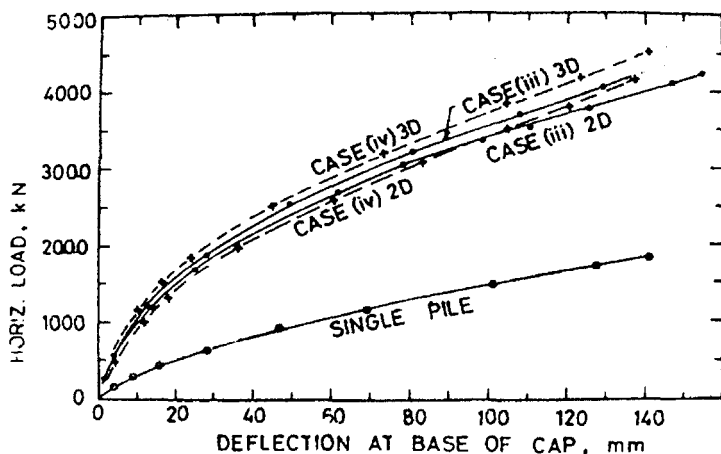


FIGURE 43 : Comparison of Three-Pile Groups

## Indian Geotechnical Centrifuge Facility

There has been a long-felt need for the creation of centrifuge facility in India for carrying out studies on scaled models of geotechnical structures. The Department of Science and Technology with cooperation from DRDO and MHRD took a lead role in supporting the establishment of the geotechnical centrifuge facility at IIT Bombay. It was soon realised for a country like India where the accent will be on infrastructure development it would be necessary to build a large size facility.

A large capacity centrifuge will allow testing of large size models making it possible to carry out studies on models of prototypes. Large model size will allow stratification of different layers and also enable extensive instrumentation. It would be easy to carry additional payload due to earthquake simulator. Also the errors associated with small machines could be considerably minimised. Keeping these requirements in perspective a geotechnical centrifuge of radius 4.5m up to the base of the basket with a payload capacity 2.5 tons at 100g has been setup at IIT Bombay. The centrifuge can operate upto 200g with reduced payload. It is proposed to equip the centrifuge with an earthquake simulator shortly. A photograph of the centrifuge is given in Plate 7. The technical details are given in Table 11.

The Centrifuge has been fabricated and erected indigenously and is now available for use. The following objectives are envisaged for this facility.

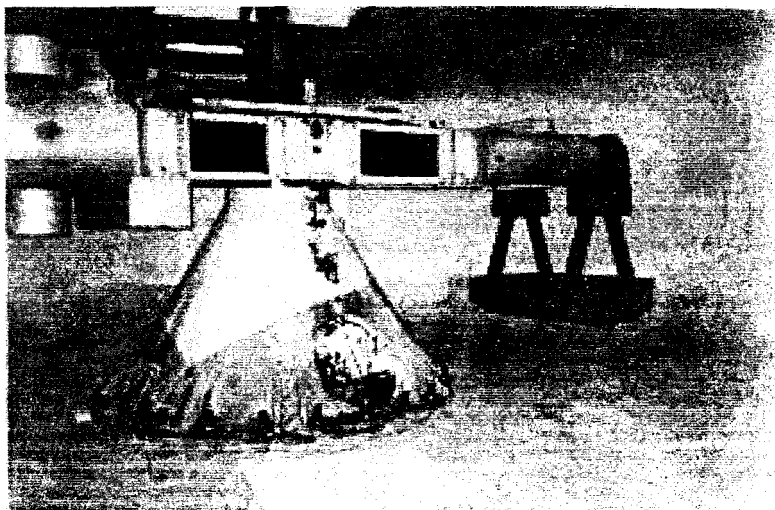


**Plate 7. Geotechnical Centrifuge at IIT Bombay**

**Table 11. The Technical Details of the Geotechnical Centrifuge at IIT Bombay**

Radius from the axis of rotation to basket base	:	4.5 m		
Acceleration range at 4.25 m radius	:	10 g to 200 g		
Maximum payload at various g-levels. Payload includes weight of strong box, Shake table, soil and other accessories for carrying out experiments but excludes the weight of swinging basket.	:			
		<u>g-level</u>	<u>Radial dist. to centre of mass of payload</u>	<u>Payload</u>
		50	4.25 m	2500 kg
		100	4.25 m	2500 kg
		200	4.25 m	625 kg
Rotational Speed of Centrifuge arm	:	46 to 205 rpm		
Speed rate stability	:	0.2 % of set rate or 0.1 rpm		
Drive system	:	450 kW DC motor		

(Table 11 Contd...)

(Table 11 Contd...)

---

Configuration	:	Swing basket at one end of the arm and adjustable counter weights at the other end.	
Static balancing of counter weight	:	Manual and motorised	
Maximum unbalance force	:	100 kN	
In-flight balancing range	:	0 to $\pm 100$ kN	
Balancing accuracy	:	$\pm 10$ kN	
In-flight balancing time	:	60 Seconds	
Soil model size	:	0.9m x 1.0m x 0.65m or 0.7m x 0.7m x 0.8m	
Basket base dimensions (clear)	:	1000 mm x 1200 mm	
Electrical slip rings	:	Video Power (220 V, 20 amp) Power (24 V, 5 amp) Transducers (10 V, 2 amp) Total :	No. 2 5 5 100 112
Hydraulic rotary joints	:	Hydraulic oil rotary joints 0 to 200 bars including 6 mm piping for fluid temperature in the range of 10 - 50° C. Air or water rotary joints 0 to 20 bars, temperature range 10-50° C. (Flow rate 10 litres/min.)	2 4
Run-up time	:	6 minutes to reach 200 g	
Run-down time	:	6 minutes from 200 g to 0	
Continuous run time	:	5 days	
Design life	:	40 years, 24,000 cycles of starting and stopping during design life.	
Environmental Sensors :		<ul style="list-style-type: none"> <li>● Temperature and humidity sensors with display at console and alarm.</li> <li>● Infra red smoke detector with alarm.</li> <li>● Unbalance sensor with display at console and alarm.</li> <li>● Acceleration sensor attached to the centrifuge base and its display.</li> <li>● Centrifuge vibration meter with alarm.</li> <li>● Microphones, amplifiers and speakers for monitoring noise inside the centrifuge chamber and the motor room.</li> </ul>	

---

- (i) The facility will be made available to other research and educational institutions and user agencies for advanced research and prototype modelling.
- (ii) To undertake basic and applied in-house research, time bound sponsored research and industrial consultancy.
- (iii) To train manpower and enable transfer of technology.

## **Concluding Remarks**

Problems of soil structure interaction can be tackled effectively by using numerical techniques incorporating appropriate constitutive models for the soil. The paper has dealt with a few of these applications pertaining to shallow and deep foundations. The predictive power of the numerical models will be enhanced by comparison of data with field measurements or with data from carefully conducted physical modelling experiments using centrifuge. It is recommended that before 1g model tests are conducted only after the similitude relationships between model and prototype are carefully evaluated and usefulness of these tests are justified.

Geotechnical Centrifuge has been accepted as a powerful tool for carrying out model studies on geotechnical structures. The important attribute of the centrifuge study is its ability to incorporate the size effect and predict the prototype behaviour. The complex stress conditions obtained in the field are well simulated in the centrifuge experiments. There is a need to acquire data from carefully conducted experiments in centrifuge simulating seismic motion. This will pave the way towards safe design of geotechnical structures to withstand earthquakes.

Numerical and centrifuge modelling are two powerful complementary technologies which can be gainfully used for tackling problems in soil-structure interaction.

## **Acknowledgement**

The Indian Institute of Technology Bombay provides the ideal ambience for academic and research activities. I have been most fortunate in being one of the members of this outstanding Institute.

Part of the of the work reported in this lecture is based on the theses of the author's students. The author wishes to thank his former students Dr.I.D.Desai, of Dr.M.M. Dewoolkar, Dr.A.D.Gadre, Shri

S.P.Khedkar, Shri. K.N.Sheth and Dr. R. Chanpura and his present student Shri S.B. Bhujbal. . The author is grateful to Prof K.R.Kulkarni for his interaction with him over the years . The collaborative work with him on pile groups has been made use of in this lecture. Prof.K.R.Kulkarni also contributed to the centrifuge project in its early stage. The work on caissons was undertaken at the initiative of Prof.R.K.Katti . A project such as the centrifuge project could only be an outcome of team effort. In this regard the author wishes to place on record and acknowledge the contributions made by his colleagues in the Geotechnical Division, Prof.G.Venkatachalam, Prof.D.M.Dewaikar, Prof.J.N.Mandal and Dr.B.V.S.Viswanadham. Expert technical assistance at various stages of project was provided by Prof. M.S.C. Bose, Prof. S.K. Pillai, Prof. U.V. Athavankar, Shri V.K. Kulkarni, Prof. G.R. Shevare, Prof. S.D. Sharma, Prof P. Vasudevan, Shri A.S. Subbiah. Assistance and supervision was provided by Shri K.G. Murumkar, Shri P.B. Bhagat. and Shri C.P. Chavan. Thanks are due to Shri V.B.Rajesh who carefully typed the manuscript.

## References

- Banerjee, P.K. and Davies, T.G. (1978) : The Behaviour of Axially and Laterally Loaded Single Piles Embedded in Nonhomogeneous Soils. *Geotechnique* (28), 3, pp.309-326.
- Bowles, J.E. (1988) : *Foundation Analysis and Design*, McGraw-Hill Book Company. New York, pp.1004.
- Buragohain, D.N. and Shah, V.L. (1981) : Finite Element Analysis of Plates of Arbitrary Shapes on Elastic Half Space. *Proc. Int. Conf. on Numerical Methods for Coupled Problems*, Swansea, pp.665-674.
- Chandrasekaran, V.S. and Khedkar, S.P. (1977) : Shear Wall Foundation Interaction, *Proc. International Symposium on Soil-Structure Interaction*, University of Roorkee, Roorkee.pp.123-127.
- Chandrasekaran, V.S. and Ambadker, A.M. (1983) : Behaviour of Axially Loaded Piles in Layered Media. *Proc. Indian Geotechnical Conference-83*, Madras, pp.II-63-67.
- Chandrasekaran, V.S., Kulkarni, K.R., and King, G.J.W. (1984) : Analytical and Centrifuge Studies on Laterally Loaded Single Piles. *Proc. Int. Symp. on Advances in Geotechnical Centrifuge Modelling*, University of California, Davis, U.S.A.

Chandrasekaran, V.S., Kulkarni, K.R. and Sheth, K.N. (1987) : Analysis of Axially Loaded Piles: Proc. IGC-87, *Indian Geotechnical Conference*, Bangalore. pp.141-145.

Chandrasekaran, V.S. and Gadre, A.D. (1994) : Role of Numerical Method in Centrifuge Modelling. *National Workshop on Numerical and Analytical Methods in Geotechnical Engineering*, IIT Delhi.

Cheung, Y.K. and Zienkiewicz, O.C. (1965) : Plates and Tanks on Elastic Foundations-An Application of Finite Element Method. *Int. J. Solids Structures*, 1: pp.451-461.

Cheung, Y.K. and Nag, D.K. (1968) : Plates and Beams on Elastic Foundations-linear and Non-linear Behaviour, *Geotechnique*, vol.18, No.2, pp.250-260.

Desai I.D. (1983) : A Finite Element Study of the Behaviour of Caisson Foundations Under Axial and Lateral Loads. *Ph.D. Thesis* submitted to Indian Institute of Technology, Bombay, pp 358.

Desai, I.D. and Chandrasekaran, V.S. (1985) : Axially Loaded Caisson Foundation, *International Journal of Structures*, vol.5, No.4.

Desai, I.D. and Chandrasekaran, V.S. (1985) : Semi-analytical Approach to No-contact Tension Problems, *2nd International Conference on Numerical Models in Geomechanics*, University of Ghent, Belgium.

Desai, I.D. and Chandrasekaran, V.S. (1986) : Semi-analytical Finite Element Procedure for Non-linear Material Behaviour, *Computers and Structures*, Vol.23.

Desai, I. D. and Chandrasekaran, V.S. (1993) : New Technique of Non-linear Finite Element Analysis for Caisson Foundation. *Proc. of the Second Asian-Pacific Conference on Computational Mechanics*, Sydney, N.S.W. Australia.

Dewoolkar, M.M. (1992) : Studies in a small Geotechnical Centrifuge. *M.Tech. Dissertation*, submitted to Indian Institute of Technology, Bombay. pp.164.

Gadre, A.D. (1992) : Assessment of Modelling Errors in Centrifuge Due to Variable Acceleration Field and Preliminary Studies on Tunnels and Footing in a Small Centrifuge. *M.Tech. Dissertation*, submitted to Indian Institute of Technology, Bombay. pp.134.

Hetenyi, M. (1946) : *Beams on Elastic Foundations*, The Univ. of Michigan Press, Ann Arbor, MI, pp.255.

King, G.J.W. and Chandrasekaran, V.S. (1974) : Interactive analysis of Rafted Multi-storey Space Frame Resting on an Inhomogeneous Clay Stratum. *Proc. International Conf. on Finite Element Methods in Engineering*, The University of New South Wales, Australia, pp.493-509.

King, G.J.W. and Chandrasekaran, V.S. (1977) : Interactive Analysis Using Simplified Soil Model, *Proce. of the International Symposium on Soil-Structure Interaction*, University of Roorkee, pp.93-99.

King, G.J.W., Dickin, E.A. and Lyndon, A. (1984) : The development of a Medium Size Centrifugal Testing Facility. *Proc. Sym. on the Application of Centrifuge Modelling to Geotechnical Design*. University of Machester, U.K., pp.25-46.

Kulkarni, K.R., Chandrasekaran, V.S. and King G.J.W., (1985), Centrifugal Model Studies on Laterally Loaded Pile Groups in Sand, *Proc. 11th Int. Conf. on Soil Mech. and Found. Eng.*, Vol. 2, pp. 1113-1116.

Matlock, H.S. and Reese, L.C. (1960) : Generalised Solutions for Laterally Loaded Piles. *J.Soil Mech. and Found. Dig.*, ASCE, 86 (SM5), pp.63-91.

O'Neill, M.W. and Ghazzaly, O.I. (1977) : Analysis of Three Dimensional Pile Groups with Nonlinear Soil Response and Pile-soil-pile Interaction. *9th Annual OTC*, Houston, Texas, pp.245-250.

Ovesen, N.K. (1980) : Discussion : The use of Physical Models in Design. *Proc. 7th Eur. Regional Conf. Soil Mech. Found. Eng.*, Brington. British Geotechnical Society, London. Vol.4, pp.315-323.

Poulos, H.G. and Davis, E.H. (1968) : The Settlement Behaviour of Single Axially Loaded Incompressible Piles and Piers. *Geotechnique* 18, pp.351-371.

Poulos, H.G. (1971) : Behaviour of Laterally Loaded Piles, I Single Piles. *J.Soil Mech. Fdn. Div.*, ASCE (97), SM5, pp.733-751.

Poulos, H.G. (1971) : Behaviour of Laterally Loaded Piles, II-pile Groups. *J. Soil Mech. Fdn. Div.* ASCE (97), SM5, pp.733-751.

Randolph, M.F. and Wroth, C.P. (1978) : Analysis of Deformation of Vertically Loaded Piles. *J. Geotech. Engng. Div., ASCE*, 104 (GT12), pp.1465-1488.

Randolph, M.F. (1981) : The Response of Flexible Piles to Lateral Loading *Geotechnique*, 31 (2), pp.247-259.

Skempton, A.W. and Bishop, A.W. (1957) : A Contribution to the Settlement Analysis of Foundations on Clay, *Geotechnique* 7, 168.

Svec, O.J. and McNiece, G.M. (1972) : Finite Element Analysis of Finite Sized Plates Bonded to an Elastic Half-space, *Computer Methods in Applied Mechanics and Engineering*, Vol.1, pp.265-277.

Reese, L.C. and Matlock, H. (1956) : Non-dimensional Solutions for Laterally Loaded Piles with Soil Modulus Proportional to Depth, *Proc. 8th Texas Conf. SMFE*, pp.1-41.

Taylor, R.N. (1995) : *Geotechnical Centrifuge Technology*, Blackie Academic & Professional. pp.1-296.

Terzaghi, K. (1955) : Evaluation of Coefficient of Subgrade Reaction, *Geotechnique*, vol.5, No.4. pp.297-326.

Vesic, A.C. (1961) : Beams on Elastic Subgrade and the Winkler's Hypothesis, *5th ICSMFE*, vo.1. pp.845-850.

Wilson, E.L. (1965) : Structural Analysis of Axi-Symmetric Solids, *Journal of the American Institute of Aeronautics and Astronautics*, 3, 12, pp.2269-2274.